

1

1 **Glucose Transporter Expression and Regulation Following a Fast**
2 **in the Ruby-throated Hummingbird, *Archilochus colubris*.**

3 Raafay S. Ali^{1,2}, Morag F. Dick², Saad Muhammad^{1,2}, Dylan Sarver³, G. William Wong³, and
4 Kenneth C. Welch Jr.^{1,2}

5 ¹ Cell and Systems Biology, University of Toronto, 25 Harbord St, Toronto, ON, Canada M5S
6 3G5

7 ² Department of Biological Sciences, University of Toronto Scarborough Campus, 1265 Military
8 Trail, Toronto, ON, Canada, M1C 1A4

9 ³ Department of Physiology, Johns Hopkins School University School of Medicine, 725 North
10 Wolfe Street Physiology 202, Baltimore, MD, United States of America, 21205

11

12 Corresponding author email: kwelch@utsc.utoronto.ca

13 Keywords: hummingbird, glucose transporter, plasma membrane, glucose, fructose

14 Summary statement: Hummingbird ingest nectar rich in glucose and fructose. When fasted,
15 tissue capacity for circulating glucose import declines while remaining elevated for fructose.
16 This may underlie maintenance of high blood glucose and rapid depletion of blood fructose.

17 **Abstract**

18 Hummingbirds subsist almost exclusively on nectar sugar and face extreme challenges
19 blood sugar regulation. Transmembrane sugar transport is mediated by facilitative glucose
20 transporters (GLUTs) and the capacity for sugar transport is dependent on both the activity of
21 GLUTs and their localisation to the plasma membrane (PM). In this study, we determined the
22 relative protein abundance in whole-tissue (WT) homogenates and PM fractions via immunoblot
23 using custom antibodies for GLUT1, GLUT2, GLUT3, and GLUT5 in flight muscle, heart, and,
24 liver of ruby-throated hummingbirds (*Archilochus colubris*). GLUTs examined were detected in
25 nearly all tissues tested. Hepatic GLUT1 was minimally present in WT homogenates and absent
26 in PM fractions. GLUT5 was expressed in hummingbird flight muscles at levels comparable to
27 that of their liver, consistent with the hypothesised uniquely high fructose-uptake and oxidation
28 capacity of this tissue. To assess GLUT regulation, we fed ruby-throated hummingbirds 1M
29 sucrose *ad libitum* for 24 hours followed by either 1 hour of fasting or continued *ad libitum*
30 feeding until sampling. We measured relative GLUT abundance and concentrations of
31 circulating sugars. Blood fructose concentration in fasted hummingbirds declined from ~5mM to
32 ~0.18mM, while fructose-transporting PM GLUT2 and PM GLUT5 did not change in
33 abundance. Blood glucose concentrations remained elevated in both fed and fasted
34 hummingbirds, at ~30mM, while glucose-transporting PM GLUT1 and PM GLUT3 in the flight
35 muscle and liver, respectively, declined in fasted birds. Our results suggest that glucose uptake
36 capacity is dynamically reduced in response to fasting, allowing for maintenance of elevated
37 blood glucose levels, while fructose uptake capacity remains constitutively elevated promoting
38 depletion of blood total fructose within the first hour of a fast.

39 **List of Abbreviations**

40 **AIC** Akaike Information Criterion

41 **AICc** Akaike Information Criterion for small sample sizes

42 **ANOVA** Analysis of Variance

43 **APS** Ammonium Persulfate

44 **cdNA** Complementary Deoxyribonucleic Acid

45 **CO₂** Carbon Dioxide

46 **DTT** Dithiothreitol

47 f_{exo} Proportion of expired CO₂ fuelled by oxidation of exogenous sugar

48 **GAPDH** Glyceraldehyde-3-Phosphate Dehydrogenase

49 **GLUT** Glucose Transporter

50 **HEK293T** Homo sapiens Embryonic Kidney cell line with Mutant SV40 large T antigen

51 **HRP** Horseradish Peroxidase

52 **LC MRM/MS** Liquid Chromatography Multiple Reaction Monitoring Mass
53 Spectrometry

54 **LMM** Linear Mixed-effects Model

55 **mM** Millimolar

56 **mRNA** Messenger Ribonucleic Acid

57 **MW** Molecular Weight

58 **NCBI** National Center for Biotechnology Information

59 **NP-40** Nonidet P-40

60 **PBST** Phosphate Buffered Saline with Tween 20

61 **PM** Plasma Membrane

62 **PVDF** Polyvinylidene Fluoride

63 **QQ plot** Quantile-quantile plot

64 **RIPA** Radioimmunoprecipitation Assay

65 **SDS** Sodium Dodecyl Sulfate

4

- 66 **SDS PAGE** Sodium Dodecyl Sulfate Polyacrylamide Gel Electrophoresis
- 67 **TEMED** Tetramethylethylenediamine
- 68 **TMIC** The Metabolomics Innovation Centre
- 69 **UTSC** University of Toronto Scarborough Campus
- 70 **WT** Whole Tissue

71 **Introduction**

72 Hummingbirds primarily subsist on a diet of floral nectar high in sucrose, glucose, and
73 fructose (del Rio et al., 1992). They are capable of oxidising glucose, fructose, or both, to power
74 their characteristic hovering behaviour (Chen and Welch, 2014). When blood sugar
75 concentrations are elevated, hummingbirds rely exclusively on these exogenous sugars to fuel
76 nearly all the metabolic needs of their active cells (Welch et al., 2018). As such, they exhibit
77 remarkable adaptations that enhance both the capacity for immediate rapid uptake and
78 metabolism and the long-term storage of these sugars (Price et al., 2015; Welch et al., 2018).
79 When possible, circulating sugars are incorporated into hummingbirds' fat stores through *de-*
80 *novo* lipogenesis by their liver (Suarez et al., 1988). As hummingbirds enter periods of
81 hypoglycaemia, such as sleeping or fasted states, the entirety of their metabolic fuel source
82 switches from circulating sugars to triglycerides derived from these fatty-acid stores (Eberts et
83 al., 2019; Suarez et al., 1990). This switch is rapid, and a transition back to sugar metabolism
84 occurs within a few minutes of sugar ingestion (Suarez and Welch, 2017). Furthermore, the
85 switch from reliance on lipid oxidation to carbohydrate oxidation is nearly complete, such that
86 mixed fuel-use does not occur for very long in hummingbirds with access to sufficient floral
87 nectar (Welch et al., 2018).

88 Hummingbird digestive physiology facilitates rapid sugar transport across the intestinal
89 lumen and into circulation (Karasov, 2017). A high cardiac output and capillary-to-muscle-fibre
90 ratio ensures high transport capacity of sugars to the site of active cells (Mathieu-Costello et al.,
91 1992; Suarez, 1992). Sugars are then facilitatively imported across the plasma membrane (PM)
92 of active cells (Suarez and Welch, 2011). Here, *in-vitro* studies of hummingbird muscle cells
93 have demonstrated that the phosphorylation capacity of cytosolic kinases for glucose appears
94 sufficient in providing energy for sustained hovering, although this may not be true for fructose
95 (Myrka and Welch, 2018). As both delivery to and phosphorylation of glucose within muscles
96 operate at rates near the theoretical maximum in vertebrates (Suarez et al., 1988; Suarez and
97 Welch, 2017) it is likely that regulation at the site of import itself exerts a great deal of control
98 over the flux through the entirety of the sugar oxidation cascade. Along with delivery and
99 phosphorylation, the sugar import step is a rate-limiting process in the paradigm outlined by
100 Wasserman et al. (2011) and is nearly entirely dependent on the presence and distribution of

101 active glucose transporters (GLUTs) (Wasserman, 2009). These proteins are a family of
102 transmembrane solute transporters (Mueckler and Thorens, 2013).

103 Studies of mammalian GLUTs demonstrate that their expression in the PM is regulated
104 by a variety of intra- and extracellular factors, including blood sugar and insulin concentrations,
105 exercise, and stress (Egert et al., 1999; Guma et al., 1995; Yang and Holman, 1993). The
106 expression and functional distribution and regulation of hummingbird GLUTs, however, remains
107 relatively unknown. Studies on GLUT isoforms of the closest relatively well-examined avian
108 species, the chicken (*Gallus gallus domesticus*), are fragmented and the distribution of avian
109 GLUT isoforms is not fully understood (Byers et al., 2018; Suarez and Welch, 2011; Sweazea
110 and Braun, 2006). It is known that chicken GLUT1 and GLUT3 share sequence homologies of
111 ~80% and ~70%, respectively, with human GLUTs, but other isoforms such as GLUT2 and
112 GLUT5 only share ~65% and ~64% sequence homology (calculated via NCBI BLAST (Boratyn
113 et al., 2012), summarised in Table S6). It is also clear that they are regulated very differently in
114 each class (Wagstaff and White, 1995; Yamada et al., 1983). Despite this, the literature on
115 mammalian GLUTs provides a useful foundation for understanding the affinities and ligand-
116 specificity of avian, including hummingbird, GLUTs. In mammals, GLUT3, followed by
117 GLUT1, show the highest affinities for glucose; $K_m \approx 1.5\text{mM}$ (Thorens and Mueckler, 2010) and
118 $K_m \approx 3\text{-}5\text{mM}$ (Zhao and Keating, 2007), respectively. GLUT5 transports fructose ($K_m \approx 11\text{-}$
119 12mM ; Douard and Ferraris, 2008), and is largely found in mammalian enteric and renal tissue
120 (Douard and Ferraris, 2008), although some presence in hepatic tissue has also been noted
121 (Godoy et al., 2006; Zhao et al., 1993). GLUT2, uniquely, shows affinity for both sugars. While
122 its affinity for glucose and fructose ($K_m \approx 17\text{mM}$ and $K_m \approx 76\text{mM}$, respectively; Zhao and
123 Keating, 2007) is relatively low compared to other isoforms, it plays a dominant role in hepatic
124 sugar transport (Wood and Trayhurn, 2003).

125 Importantly, it is only when GLUT isoforms are expressed and active in the PM that
126 transmembrane sugar transport can occur from the blood into the active cell (Guma et al., 1995;
127 Wasserman, 2009; Yamada et al., 1983). In mammals, GLUT4 translocation to the PM by
128 insulin-stimulation following feeding is known to recruit other GLUT isoforms to the PM as
129 well, increasing the sugar import rate into active cells (Guma et al., 1995). Hummingbirds
130 (Welch et al., 2013), much like chickens (Byers et al., 2018), do not express transcript or protein
131 of the insulin-sensitive GLUT4 isoform. Chicken insulin levels do not significantly change with

132 dietary status (Simon et al., 2011), and this is presumably also true in hummingbirds. Further,
133 circulating insulin does not significantly increase sugar import in chicken muscles (Chen, 1945),
134 though it may in the liver (Dupont, 2009; Zhang et al., 2013). Lastly, and unlike mammals,
135 hummingbirds have limited intramuscular glycogen stores (Suarez et al., 1990), and therefore
136 rely on newly imported sugars from circulation for carbohydrate oxidation (Welch et al., 2018).
137 Despite missing critical elements of the insulin-GLUT4 pathway, fed hummingbirds utilise
138 circulating sugars, when available, at very high rates to meet their metabolic demands (Suarez
139 and Welch, 2017).

140 Previous studies have confirmed the presence of GLUT1 and GLUT5 transcript in nearly
141 all hummingbird tissue examined (Myrka and Welch, 2018). Immunohistochemistry of
142 hummingbird myocytes using a commercial antibody for GLUT1 have also shown GLUT1
143 localisation to the PM (Welch et al., 2013), though, the results were not definitive. In this study,
144 using custom antibodies for the different isoforms of hummingbird GLUTs, we sought to
145 identify the tissue-specific protein distribution and to quantify the abundance in the PM, of
146 GLUT1, GLUT2, GLUT3, and GLUT5. We predicted GLUT1 would be detected in
147 hummingbird flight muscle, cardiac, and liver tissue, in accordance with its ubiquitous presence
148 in mammalian tissue (Mueckler and Thorens, 2013), as well as its previous detection in
149 hummingbird myocytes (Welch et al., 2013). As GLUT2 plays a stronger role in enteric
150 (Karasov, 2017) and hepatic (Mueckler and Thorens, 2013) sugar transport, we predicted that its
151 abundance would be limited in muscles and more predominantly found in the liver. In mammals,
152 GLUT3 is observed in close association with GLUT1 (Simpson et al., 2008) and may function as
153 a replacement for GLUT4 in certain muscle developmental stages (Klip et al., 1996). We
154 expected to detect GLUT3 in tissues also expressing GLUT1. We also expected to find GLUT5
155 in both the liver and muscles, as hummingbird muscles are capable of supporting hovering flight
156 on fructose-only meals (Chen and Welch, 2014). To further characterise the regulatory aspects of
157 hummingbird GLUTs, we compared the abundance of GLUT1, GLUT2, GLUT3, and GLUT5 in
158 the PM of fed and fasted hummingbirds. We also measured levels of circulating glucose and
159 fructose in these birds. Based on previous measurements of hummingbird blood glucose
160 (Beuchat and Chong, 1998), we expected to see high levels of glucose (~40mM) in the fed
161 condition and lower levels in the fasted (~15mM). Previous measurements of hummingbird
162 blood fructose have not been made. However, similar to that of frugivorous bats (Keegan, 1977),

163 we predicted blood fructose concentrations in fed hummingbirds to be ~5-10mM in fed and
164 ~0mM in fasted hummingbirds. Given the rapid switching between glucose or fructose oxidation
165 and oxidation of lipid stores in foraging versus fasting hummingbirds, we expected a greater
166 abundance of PM GLUT1, PM GLUT3, and PM GLUT5 in flight muscle and liver of fasted
167 hummingbirds. Finally, we expected little difference in between GLUT2 abundance in the PM of
168 tissue from fed and fasted hummingbirds.

169

Materials and Methods

170 1.1 Animal Use and Ethics Statement.

171 This study was approved and performed adhering to the requirements of the University of
172 Toronto Laboratory Animal Care Committee and the Canadian Council on Animal Care. Twelve
173 adult male ruby-throated hummingbirds (*Archilochus colubris*) were captured in the early
174 summer at the University of Toronto Scarborough (UTSC) using modified box traps and housed
175 individually in Eurocages (Corners Ltd, Kalamazoo, MI, USA) in the UTSC vivarium. They
176 were provided with perches and fed on a maintenance diet of NEKTON-Nectar-Plus (Keltern,
177 Germany).

178 All hummingbirds were provided with a sucrose solution for 24 hours prior to the experiment.
179 Birds were divided into a fed group (n = 6), which was provided with *ad-libitum* 1M sucrose
180 solution up to sampling, beginning at 10AM, and a fasted group (n = 6), which was deprived of
181 any food for a 1 hour duration prior to the 10AM sample collection. To minimize interindividual
182 variation in activity level and energy expenditure, birds from both treatment groups were held in
183 small glass jars, perched on wooden dowels, in which they were constrained from flying, for the
184 duration of the 1 hour fast. Respirometry measurements by Chen and Welch (2014) have
185 previously shown that this is sufficient time for the fasted hummingbirds to shift from fuelling
186 metabolism with circulating sugars to fats. Fed hummingbirds will continue to exclusively
187 metabolise sugars. Hummingbirds were then anaesthetised with isoflurane inhalation and
188 euthanized via decapitation. Immediately after decapitation, blood was sampled from the carotid
189 artery using heparinized capillary tubes and spun at 3800 g for 10 minutes at room temperature
190 and the plasma stored at -80 °C. Flight muscle (the pectoralis and supracoracoideus muscles),
191 heart, and liver were extracted and frozen with isopentane cooled with liquid nitrogen. All tissues
192 were stored at -80 °C.

193 1.2 Circulating Sugar and Metabolite Analysis.

194 Plasma samples were sent to the Metabolomics Innovation Centre (TMIC) at the University of
195 Victoria (Victoria, British Columbia, Canada) to be analyzed via service 45 (absolute
196 quantitation of central carbon metabolism metabolites and fructose) found here:
197 <https://www.metabolomicscentre.ca/service/45>. Quantitation of glucose and fructose

198 concentrations in plasma samples was achieved via chemical derivatization – liquid
199 chromatography – multiple reaction monitoring/mass spectrometry (LC-MRM/MS) following a
200 protocol outlined by Han et al. (2016). Quantitation of central carbon metabolites (organic acids;
201 lactate and pyruvate) was done via the protocol outlined by Han et al. (2013).

202 1.3 Antibody Design, Production, and Isoform Specificity

203 Anti-rabbit polyclonal antibodies for GLUT isoforms were designed in conjunction to minimise
204 cross-reactivity using the services of Pacific Immunology (Ramona, CA, USA). Epitope design
205 was accomplished using messenger RNA (mRNA) sequences for ruby-throated hummingbird
206 GLUT isoforms 1, 2, 3, and 5 that were obtained from the hummingbird liver transcriptome
207 (Workman et al., 2018). The concentration of the affinity-purified antibody samples was
208 assessed using ELISA by Pacific Immunology (ab-GLUT1 $\approx 1.1 \text{ mg}\cdot\text{ml}^{-1}$, ab-GLUT2 ≈ 5.7
209 $\text{mg}\cdot\text{ml}^{-1}$, ab-GLUT3 $\approx 2.6 \text{ mg}\cdot\text{ml}^{-1}$, ab-GLUT5 $\approx 1.0 \text{ mg}\cdot\text{ml}^{-1}$). The final experimental dilutions
210 were determined empirically through preliminary experiments and are provided below.

211 1.3.1 Generation of mammalian expression plasmids encoding *A. colubris* GLUT1, GLUT2, 212 GLUT3, and GLUT5.

213 The cDNA encoding *A. colubris* GLUT1 (NCBI Accession Number MT472837), GLUT2
214 (MT472838), GLUT3 (MT472839), and GLUT5 (MT472840) were synthesized by GenScript
215 based on the full-length mRNA sequences derived from our previously published RNA
216 sequencing data (Workman et al., 2018). The V5 epitope tag (encoding the peptide
217 “GKPIP NPLLGLDST”) was inserted at the 3’ end of each cDNA immediately after the last
218 coding amino acid. All epitope-tagged cDNA sequences were cloned into the EcoRI restriction
219 site of the mammalian expression vector, pCDNA3.1 (+) (Invitrogen). All expression plasmids
220 were verified by DNA sequencing.

221 1.3.2 Specificity immunoblots

222 SDS-PAGE was run on cell lysates of HEK293T cells transiently transfected, using
223 lipofectamine 2000 (Invitrogen), with hummingbird GLUT1, GLUT2, GLUT3, or GLUT5
224 (acGLUT1, GLUT2, GLUT3, or GLUT5) expression vectors; all containing a V5 tag. Cell
225 lysates produced using RIPA buffer (50 mM Tris-HCl, pH 7.4; 150 mM NaCl; 1 mM EDTA;
226 1% Triton X100; 0.25% deoxycholate) supplemented with protease and a phosphatase inhibitor
227 cocktail (MilliporeSigma, Burlington, Massachusetts, USA and Roche, Basel, Switzerland;

228 respectively). Each lysate was confirmed to express the appropriate recombinant protein at the
229 expected size using an anti-V5 antibody produced in rabbit (Sigma V8137). Isoform specificity
230 was tested via immunoblotting all cell lysates (empty vector control, acGLUT1, GLUT2,
231 GLUT3, and GLUT5) with each novel acGLUT antibody and observing GLUT protein signal
232 overlap; none was observed. Briefly, each immunoblot lane represents a cell lysate produced
233 from an entire well of a 6-well cell-culture dish (Thermo Scientific, Nunc). Lysates were diluted
234 with SDS loading dye (final concentration: 50 mM Tris-HCl, pH 7.4, 2% SDS, 6% glycerol, 1%
235 2-ME, and 0.01% bromophenol blue) and not boiled. An equal volume of each lysate was added
236 to the designated lane on a 12% polyacrylamide gel (Bio-Rad, Hercules, CA, USA) and
237 separated by electrophoresis. The BioRad Trans-Blot Turbo semidry system was used to transfer
238 protein onto PVDF membranes. Blots were blocked in 5% non-fat milk in Phosphate buffered
239 saline with Tween 20 (PBST) and exposed to primary antibodies overnight at 4°C. After
240 washing, blots were exposed to HRP-conjugated secondary antibody (Anti-Rabbit IgG, 7074S,
241 Cell Signaling Technology, Danvers, MA, USA) for 1 h at room temperature and developed in
242 ECL (Amersham ECL Select; GE Healthcare, Chicago, IL, USA). Bands were visualized with
243 the MultiImage III FluorChem Q (Alpha Innotech, San Leandro, CA, USA). Primary antibodies
244 were diluted 1:1000 in PBST + 0.02% sodium azide. The secondary antibody was diluted
245 1:10,000 in PBST + 0.02% sodium azide.

246 1.4 Tissue Sample Preparation.

247 Each sample underwent either a plasma membrane fractionation protocol established by
248 (Yamamoto et al., 2016) and slightly modified by replacing NP-40 (nonidet P-40) with Triton X-
249 100 (Sigma-Aldrich, St. Louis, Missouri) to obtain only PM-proteins, or a
250 radioimmunoprecipitation assay buffer (RIPA) homogenisation (part of the same protocol) to
251 obtain all proteins contained in a whole-cell. Fractionation used different detergent
252 concentrations (0.1%, 1%, 2%) in the homogenisation buffers to solubilise proteins and create
253 protein-detergent complexes depending on whether they are in the hydrophilic (cytosolic)
254 domain or the hydrophobic (PM) domain.

255 1.3.3 Buffer composition.

256 Buffer A01 (0.5M DTT, ddH₂O, and 0.1% v/v Triton X-100), A1 (0.5M DTT, ddH₂O, and 1%
257 v/v Triton X-100), and 2× RIPA (20mM Tris-HCl, pH 8.0, 300mM NaCl, 2% v/v Triton X-100,

258 1% w/v sodium deoxycholate, 0.2% w/v sodium dodecyl sulfate (SDS), 1mM DTT) were
259 prepared. All reagents were cooled to 4°C before homogenisation and included Sigma P8340
260 protease inhibitor cocktail.

261 1.3.4 Homogenisation and plasma membrane fractionation.

262 20 mg of flight muscle, liver, or heart was cut on a cold aluminum block and immediately placed
263 in an ice-bath. The tissue was minced in buffer A01 with scissors and homogenised using a
264 VWR handheld pestle homogenizer (BELAF650000000) The homogenate was passed through a
265 21G needle three times to liberate nuclear and intracellular proteins. An aliquot of the
266 homogenate was left on ice for 60 minutes in 2× RIPA buffer. This whole-tissue RIPA-fraction
267 was then centrifuged at 12,000g for 20 minutes at 4°C, allowing proteins to be solubilised. The
268 supernatant was collected and stored at -80°C as the whole-tissue (WT) homogenate. The
269 remainder of the homogenate was centrifuged at 200g for 1 min at 4°C. The upper phase was set
270 aside, and 90µL of buffer AO1 was added to the lower phase which was homogenised for 10s.
271 The lower phase was centrifuged at 200g for 1 minute and added to the tube containing the upper
272 phase. The combined phases were centrifuged at 750g for 10 minutes. The supernatant consisting
273 of non-PM proteins was removed. The remainder of the protein-detergent complexed pellet was
274 resuspended with and kept on ice for 60 minutes. After centrifugation at 12000g for 20 minutes,
275 and the supernatant containing only PM-associated proteins was collected as the “plasma
276 membrane fraction”.

277 1.5 SDS-PAGE.

278 10% resolving and 4% stacking gels were cast using a 15-well comb and the AA-Hoefer Gel
279 Caster Apparatus (10%; 33% 30%-Acrylamide (37.1:1), 33% Separating gel buffer (1.5 M Tris
280 Cl, 0.4% SDS), 55% ddH₂O, 0.65% ammonium persulfate (APS), 5.5% TEMED), (4%; 13.4%
281 30%-Acrylamide, 9.3% Stacking gel buffer (0.5 M Tris Cl, 0.4% SDS), 33% ddH₂O, 0.06%
282 APS, 3.3% TEMED). Samples were incubated in a 1:1 (w/v) ratio of 2× sample buffer (0.2M
283 DTT, BioRad Laemmli Sample Buffer #1610737) at room temperature for 20 minutes. The AA-
284 Hoefer SE600 Vertical Gel Electrophoresis apparatus was set up with 6L running buffer (10%
285 BioRad 10× Tris/Glycine/SDS #1610732, 90% ddH₂O). The gel was run at 90V for 20 minutes
286 and 110V for another 75 minutes with power supplied from an AA-Hoefer PS200HC Power
287 Unit.

288 1.4.1 Electroblood and immunoblot

289 The SDS-PAGE gel was transferred to 0.45µm pore nitrocellulose (NC) membrane (GE Life
290 Sciences #10600003 Protran Premium 0.45 NC) using the AA-Hoefer TE22 Mighty Small
291 Transfer unit at 110V for 90 minutes with water cooling and immersion in an icebath. The
292 transfer buffer consisted of 192mM glycine, 24.8mM Tris, 0.00031% SDS, 20% methanol. To
293 normalise, a total-protein stain, SYPRO Ruby Red Blot (BioRad #1703127), was used and
294 imaged on a Bio-Rad PharosFX Molecular Imager (#1709460) using a 532nm laser and captured
295 with a 600-630nm band pass filter. The membranes were incubated with primary antibody
296 overnight at the following dilutions in PBST (phosphate-buffered saline, 0.1% Tween-20) buffer:
297 GLUT1 (1:250), GLUT2 (1:2000), GLUT3 (1:2000), GLUT5 (1:500). Membranes were then
298 incubated with anti-rabbit horseradish-peroxidase-conjugated secondary antibody (Cell
299 Signalling Technology #7074) at 1:1000 dilution with PBST. Finally, Pierce
300 Electrochemiluminescent Reagent (Pierce 32106) was used to fluoresce conjugates which were
301 imaged using a BioRad Chemidock XRS+ Gel Imager.

302 1.6 PM fraction purity

303 To validate the separation of PM proteins from cytosolic proteins, commercially-available
304 control antibodies were used that were validated by the manufacturer for cross-reactivity in
305 chickens. Known PM-residing and cytosol-residing proteins targeted and their abundance was
306 used to assess the degree of PM fractionation in flight muscle, liver, and heart samples. The
307 membranes were incubated at 1:1000 dilution for 90 minutes at room temperature and included
308 antibodies for 1) E-cadherin (Cell Signalling Tech. 24E10), 2) Na⁺/K⁺ ATPase (Cell Signalling
309 Tech. 3010), 3) Glyceraldehyde-3-phosphate dehydrogenase (GAPDH) (Cell Signalling Tech.
310 14C10), and 4) Fatty acid translocase (FAT) (Abgent AP2883c).

311 1.7 Western Blot Band Normalisation.

312 GLUT protein molecular weights were predicted using ExPASy (Gasteiger et al., 2005). Protein
313 quantitation was done with a Pierce 660nm assay. 5µg of sample protein was loaded into each
314 well of the polyacrylamide gel, in comparison with wells containing visible protein ladder
315 (Sigma 26616). The antibody staining intensity of each Western blot sample was normalised to
316 its corresponding total-protein stain intensity using BioRad ImageLab software. Background
317 subtraction was applied to the total protein stain in a lane-wise fashion, while no background

318 subtraction was applied to the antibody staining intensity. Fluorescence intensity for the total-
319 protein stain was measured using 30% of the lane-width as per the recommendation of Gassmann
320 et al. (2009). The antibody stain was measured using a fixed lane-width comprising of the entire
321 lane. Normalised molecular weights were recorded.

322 1.8 Statistical Analysis.

323 A Student's T-test was performed for the sugar and metabolite concentrations between fed and
324 fasted hummingbirds. We evaluated variation in isoform intensity data for each GLUT by
325 creating linear mixed-effects models (LMMs) in R statistical language (version 3.6.1, r-
326 project.org) using the lme4 package (Bates et al., 2015) for GLUT isoform fluorescence intensity
327 data. We compared relative GLUT 1, 2, 3, and 5 abundance among tissues, and between fed and
328 fasted individuals using a fully factorial design. Assumptions of residual normality were checked
329 through visual inspection of the quantile-quantile (Q-Q) plot, a frequency histogram, and the
330 Shapiro-Wilk Normality Test. When necessary, model parameters were transformed by a chosen
331 function (the details of which are presented in the Results section below) resulting in the greatest
332 homoskedasticity and data was fitted using the following formula:

$$333 \quad \textit{Fluorescence Intensity} \sim \textit{Treatment} \times \textit{Tissue} + \textit{Blot}$$

334 which outperformed more simplified models, as indicated by AICc (Akaike information criterion
335 corrected for small sample sizes), the details of which are presented in Table S5. To account for
336 the contribution of blot-to-blot variation, individual blots were treated as random effects
337 (represented as *Blot* in the formula). Analysis of variance (ANOVA) was performed on the
338 model parameters to determine the significance of any interactions. Post-hoc analysis was
339 performed using the emmeans package (Lenth, 2019) within R software to determine group
340 means and standard error. Pairwise comparison was performed to determine statistical
341 significance of groups using the Tukey HSD method with the contrast function from the
342 emmeans package. All data are presented as mean \pm standard error.

343

344

Results

345 2.1 Circulating Sugars and Metabolites of Fed and Fasted Hummingbirds

346 Overall, a significant difference was only observed for blood fructose concentrations ($t_{9,9} = -17.2$,
347 $p = 0.001$) which were higher in fed hummingbirds (5.34 ± 0.2 mM) compared to fasted ($0.21 \pm$
348 0.1 mM). Glucose concentrations in fed hummingbirds (30.04 ± 2.0 mM) remained similarly
349 elevated in fasted hummingbirds (29.67 ± 1.5 mM). Lactate concentrations in fed individuals
350 (4.31 ± 1.3 mM) were slightly lower than in fasted (6.35 ± 0.9 mM) although this was not a
351 significant difference. Likewise, pyruvate concentrations in fed hummingbirds (0.21 ± 0.03 mM)
352 remained elevated in fasted hummingbirds (0.22 ± 0.01 mM). These results are summarised in
353 Figure 1.

354 2.2 Antibody Specificity and GLUT Detection

355 Antibodies showed a high degree of specificity for their isoform in immunoblots of HEK293 cell
356 lysates (Table S3). In hummingbird tissue, GLUT proteins were identified by band molecular
357 weights, and were, with one exception, present in both PM fractions and WT homogenates
358 following PM fractionation (Table S1). GLUT1, GLUT2, GLUT3, and GLUT5 were detected in
359 WT homogenates of flight muscle and heart tissue of ruby-throated hummingbirds, as well as in
360 PM fractions. GLUT1 in liver WT homogenates was minimally detected and was not detected at
361 all in liver PM fractions. GLUT1, GLUT2, and GLUT5 were detected at approximately their
362 expected molecular weights in all tissues. GLUT3 was detected at a size slightly larger than
363 predicted.

364 2.3 Relative GLUT Abundance

365 2.3.1 GLUT1

366 With regards to the WT homogenates, no significant differences were observed in the relative
367 abundance of GLUT1 among tissues ($F_{2,2.5} = 11.58$, $p = 0.055$) or the interaction of tissue and
368 treatment ($F_{2,13} = 0.262$, $p = 0.773$). While WT flight muscle, regardless of treatment, had a
369 similar GLUT1 abundance to WT heart, WT flight muscle had a significantly greater abundance
370 compared to WT liver in both fed (flight muscle / liver ratio: 4.75 ± 1.27 , $t_{3.02} = 4.54$, $p = 0.040$)
371 and fasted (flight muscle / liver ratio: 5.76 ± 1.54 , $t_{3.02} = 4.28$, $p = 0.046$) treatments. These
372 results are summarised in Table 3 and Fig. 2A. The treatment itself, fasting, did have a

373 significant effect ($F_{1,13} = 7.99, p = 0.014$) on WT GLUT1 abundance, however, multi-factor
374 multiple comparisons using the Tukey HSD method show that only flight muscle WT GLUT1
375 abundance was significantly lower in fasted hummingbirds (fasted/fed ratio: 0.73 ± 0.09 ; $t_{13} =$
376 $2.63, p = 0.021$) (Table 1). While the effect of treatment was not significant as a whole for PM
377 GLUT1 ($F_{1,13.02} = 3.74, p = 0.075$; Treatment), we did observe a significant effect of tissue ($F_{1,$
378 $3.78 = 24, p = 0.009$) and the interaction of tissue and treatment ($F_{1, 13.02} = 17.03, p = 0.012$).
379 These results are summarised in Table 4 and Fig. 2B. The relative abundance of PM GLUT1
380 was >2-fold higher in flight muscle compared to heart within the fed treatment (Fed flight
381 muscle / heart ratio: $4.87 \pm 1.31, t_{4.68} = 5.89, p = 0.009$). Additionally, PM GLUT1 abundance
382 was significantly lower in flight muscle of fasted hummingbirds (fasted/fed ratio: $0.61 \pm 0.06, t_{13}$
383 $= 4.66, p = 0.002$) (Table 2).

384 2.3.2 GLUT2

385 Amongst WT homogenates, a significant effect of treatment was observed regarding WT
386 GLUT2 relative abundance ($F_{1, 11} = 6.22, p = 0.029$). Multiple comparisons revealed that only
387 flight muscle had a significantly lower WT GLUT2 abundance in fasted hummingbirds
388 (fasted/fed ratio: $0.54 \pm 0.08, t_{14.5} = 2.63, p = 0.019$), while heart and liver tissue did not show a
389 significant difference (Table 1 and Fig. 3A). Regardless of feeding or fasting treatment, no
390 significant difference was observed in WT GLUT2 relative abundance among tissues (Table 3).
391 No significant difference in relative abundance was noted for tissue or the interaction of tissue
392 and treatment for WT GLUT2. Further, no significant difference was observed among tissues,
393 treatment, or the interaction of tissue and treatment for PM GLUT2 (Table 2, Table 4, and Fig.
394 3B).

395 2.3.3 GLUT3

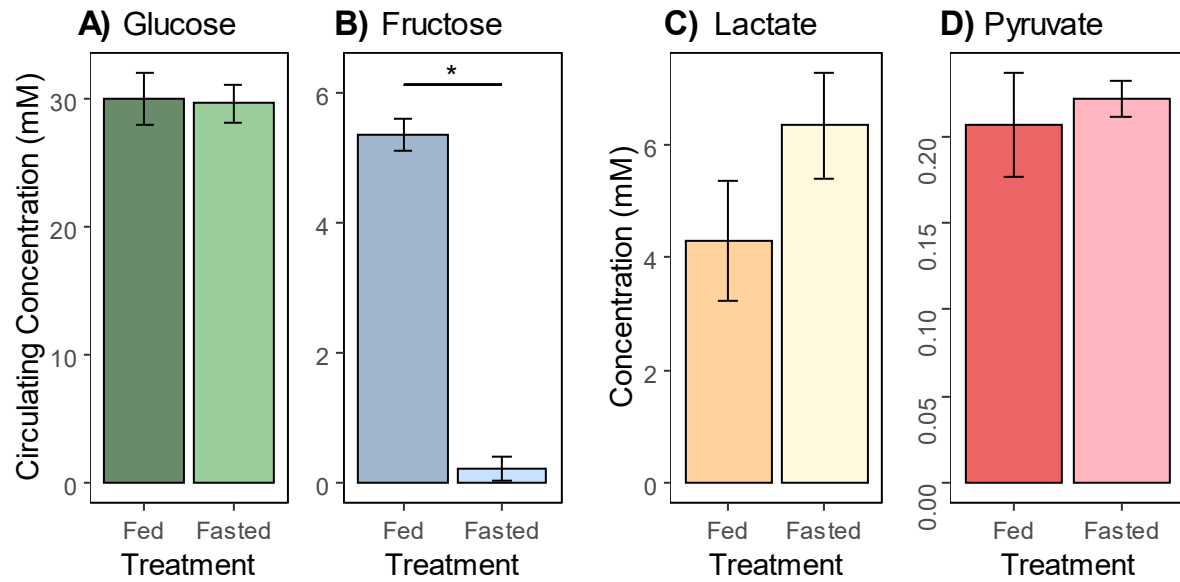
396 Fasting significantly affected the relative abundance of WT GLUT3 ($F_{1, 11} = 17.08, p = 0.002$).
397 Multi-factor multiple comparisons with the Tukey HSD method revealed that both flight muscle
398 (fasted/fed ratio: $0.68 \pm 0.09, t_{24.8} = 2.61, p = 0.015$) and liver (fasted/fed ratio: $0.58 \pm 0.09, t_{24.8}$
399 $= 4.58, p = 0.0001$) had significantly less WT GLUT3 in fasted hummingbirds, while no
400 significant difference was observed in heart WT homogenates (Table 1 and Fig. 4A). No
401 significant difference was observed for relative WT GLUT3 abundance among tissues or the
402 interaction of tissue and treatment. Regardless of treatment, WT GLUT3 abundance was similar

403 among tissues with the exception of the liver having significantly greater relative WT GLUT3
404 abundance compared to heart in fed hummingbirds (fed liver / heart ratio: 2.46 ± 0.46 , $t_{3,5} = 5.83$,
405 $p = 0.014$) (Table 3 and Fig. 4B). In PM fractions, a significant effect of the fasting treatment
406 was observed on the relative PM GLUT3 abundance ($F_{1,16} = 13.13$, $p = 0.002$). No significant
407 difference was observed among tissues (Table 4), however, the interaction of tissue and
408 treatment was significant ($F_{2,16} = 6.46$, $p = 0.009$). Through multiple comparisons, it was
409 observed that only liver PM GLUT3 relative abundance was significantly lower in fasted
410 hummingbirds (fasted/fed ratio: 0.58 ± 0.14 , $t_{16} = 4.54$, $p = 0.004$) (Table 2).

411 2.3.4 GLUT5

412 No significant effect of tissue or treatment, or their interaction, were observed for the relative
413 abundance of WT GLUT5. Regardless of treatment WT GLUT5 relative abundance did not
414 differ significantly between tissues (Table 1, Table 3, Fig. 5A). PM GLUT5 did not show any
415 significant effect with tissue, treatment, or their interaction. No significant effect was observed in
416 any tissue with fasting treatment (Table 2, Fig. 5B). Regardless of feeding or fasting, no
417 significant difference was observed in the relative PM GLUT5 abundance among tissues (Table
418 4).




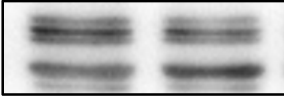

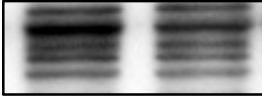
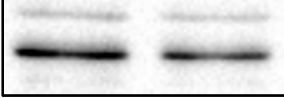

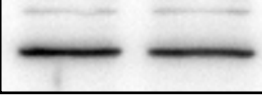

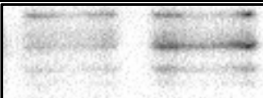
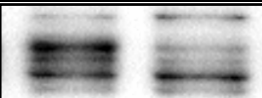
419 **Tables and Figures**




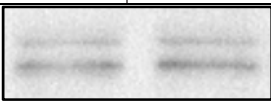

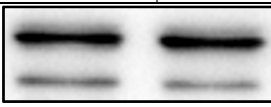
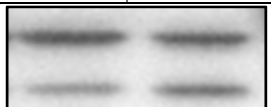

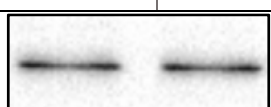
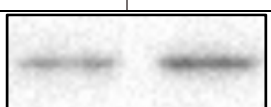
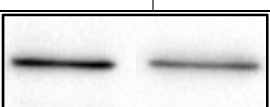
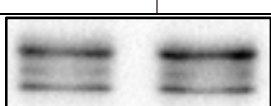
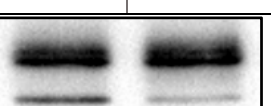

420

421 **Figure 1: Mean concentrations (mM) \pm standard error of circulating sugars A) Glucose, B)**
422 **Fructose from plasma samples and metabolites C) Lactate, D) Pyruvate from whole-tissue**
423 **homogenates of fed ($n = 6$) and fasted ($n = 5$). Data is presented as mean concentration in**
424 **millimoles \pm standard error. Asterisk (*) indicates $p = 0.001$.**

425 **Table 1: Relative WT abundance of GLUT1, GLUT2, GLUT3, and GLUT5 in flight**
 426 **muscle, heart, and liver of fed and fasted hummingbirds.** Data and representative
 427 immunoblots are presented here for the whole tissue (WT) homogenates of hummingbird tissue.
 428 Fasted/fed ratios reflect the relative variation in GLUT protein abundance with fasting treatment.
 429 Observed molecular weights (M.W.) are reported. Sample sizes are given for the number of 1)
 430 fed hummingbirds, 2) fasted hummingbirds. Asterisks (*) indicate $p < 0.05$.

Whole Tissue Homogenate	M.W. (kDa)	Flight Muscle		Heart		Liver	
		Fed	Fast	Fed	Fast	Fed	Fast
GLUT1	47.0 →						
Fasted/Fed Ratio		0.73 ± 0.09		0.81 ± 0.16		0.60 ± 0.10	
		$p = 0.010^*$	$n = 6, 6$	$p = 0.370$	$n = 2, 2$	$p = 0.126$	$n = 3, 3$
GLUT2	43.5 →						
Fasted/Fed Ratio		0.54 ± 0.08		0.75 ± 0.16		0.96 ± 0.17	
		$p = 0.019^*$	$n = 4, 4$	$p = 0.134$	$n = 2, 2$	$p = 0.786$	$n = 3, 3$
GLUT3	72.4 →						
Fasted/Fed Ratio		0.68 ± 0.09		0.82 ± 0.16		0.58 ± 0.09	
		$p = 0.015^*$	$n = 4, 4$	$p = 0.626$	$n = 2, 2$	$p = 0.0001^*$	$n = 3, 3$
GLUT5	55.3 →						
Fasted/Fed Ratio		1.11 ± 0.27		0.82 ± 0.36		1.28 ± 0.36	
		$p = 0.350$	$n = 4, 4$	$p = 0.987$	$n = 2, 2$	$p = 0.554$	$n = 3, 3$

432 **Table 2: Relative PM abundance of GLUT1, GLUT2, GLUT3, and GLUT5 in flight**
 433 **muscle, heart, and liver of fed and fasted hummingbirds.** Data and representative
 434 immunoblots are presented here for hummingbird tissue samples that underwent plasma
 435 membrane fractionation; only PM-residing GLUTs are presented. Fasted/fed ratios reflect the
 436 relative variation in GLUT protein abundance with fasting treatment. Observed molecular
 437 weights (M.W.) are reported. Sample sizes are given for the number of 1) fed hummingbirds, 2)
 438 fasted hummingbirds. Asterisks (*) indicate $p < 0.05$.

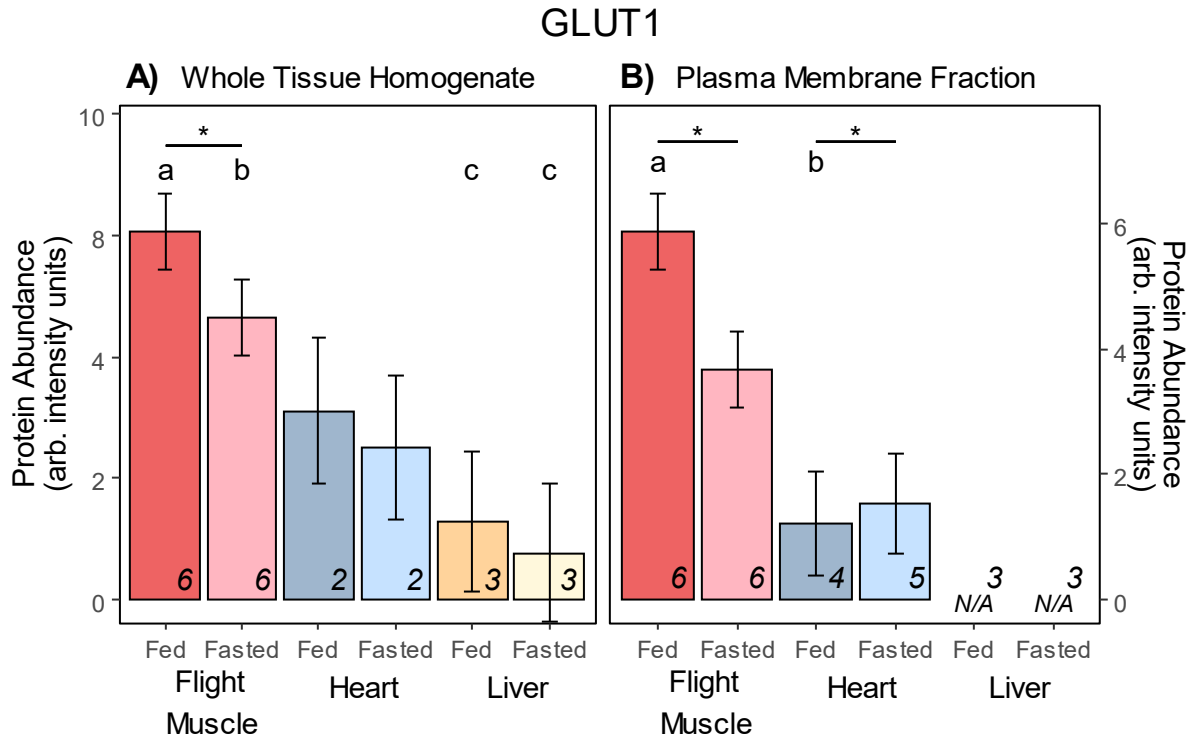
Plasma Membrane Fraction	M.W. (kDa)	Flight Muscle		Heart		Liver	
		Fed	Fast	Fed	Fast	Fed	Fast
GLUT1	47.0 →						
		Fasted/Fed Ratio		Fasted/Fed Ratio		Fasted/Fed Ratio	
		0.61 ± 0.06		1.20 ± 0.15		N/A	
		$p = 0.002^*$	$n = 6, 6$	$p = 0.500$	$n = 4, 5$	N/A	N/A
GLUT2	43.5 →						
		Fasted/Fed Ratio		Fasted/Fed Ratio		Fasted/Fed Ratio	
		0.81 ± 0.12		1.06 ± 0.14		0.96 ± 0.16	
		$p = 0.300$	$n = 4, 4$	$p = 0.584$	$n = 5, 5$	$p = 0.792$	$n = 3, 3$
GLUT3	72.4 →						
		Fasted/Fed Ratio		Fasted/Fed Ratio		Fasted/Fed Ratio	
		0.90 ± 0.14		0.99 ± 0.14		0.58 ± 0.10	
		$p = 0.903$	$n = 4, 4$	$p = 1.000$	$n = 5, 5$	$p = 0.004^*$	$n = 3, 3$
GLUT5	55.3 →						
		Fasted/Fed Ratio		Fasted/Fed Ratio		Fasted/Fed Ratio	
		0.17 ± 0.30		1.13 ± 0.26		0.89 ± 0.27	
		$p = 0.308$	$n = 4, 4$	$p = 0.864$	$n = 5, 5$	$p = 0.754$	$n = 3, 3$

440 **Table 3: Relative abundance of GLUT1, GLUT2, GLUT3, and GLUT5 among WT**
 441 **homogenates compared pair-wise between flight muscle, heart, and liver of fed and fasted**
 442 **hummingbirds.** Data represents the relative whole-tissue GLUT abundance. Asterisks (*)
 443 indicate $p < 0.05$.

Whole Tissue Homogenate	GLUT Isoform	Relative Fed Ratio	<i>p</i> -value	Sample Size	Relative Fasted Ratio	<i>p</i> -value	Sample Size
Flight Muscle / Heart	GLUT1	1.95 ± 0.54	0.082	6, 2	1.76 ± 0.49	0.120	6, 2
	GLUT2	0.70 ± 0.35	0.486	4, 2	0.37 ± 0.18	0.399	4, 2
	GLUT3	1.59 ± 0.31	0.175	4, 2	1.32 ± 0.26	0.712	4, 2
	GLUT5	1.82 ± 1.37	0.911	4, 2	2.45 ± 1.97	0.887	4, 2
Flight Muscle / Liver	GLUT1	4.75 ± 1.27	0.040*	6, 3	5.76 ± 1.54	0.046*	6, 3
	GLUT2	0.65 ± 0.32	0.386	4, 3	0.37 ± 0.12	0.068	4, 3
	GLUT3	0.65 ± 0.11	0.086	4, 3	0.75 ± 0.13	0.429	4, 3
	GLUT5	0.59 ± 0.53	0.985	4, 3	0.52 ± 0.46	0.816	4, 3
Heart / Liver	GLUT1	2.44 ± 0.83	0.147	2, 3	3.28 ± 1.11	0.075	2, 3
	GLUT2	0.93 ± 0.52	0.992	2, 3	0.73 ± 0.41	0.699	2, 3
	GLUT3	0.41 ± 0.08	0.014*	2, 3	0.57 ± 0.11	0.185	2, 3
	GLUT5	0.33 ± 0.29	0.697	2, 3	0.21 ± 0.20	0.350	2, 3

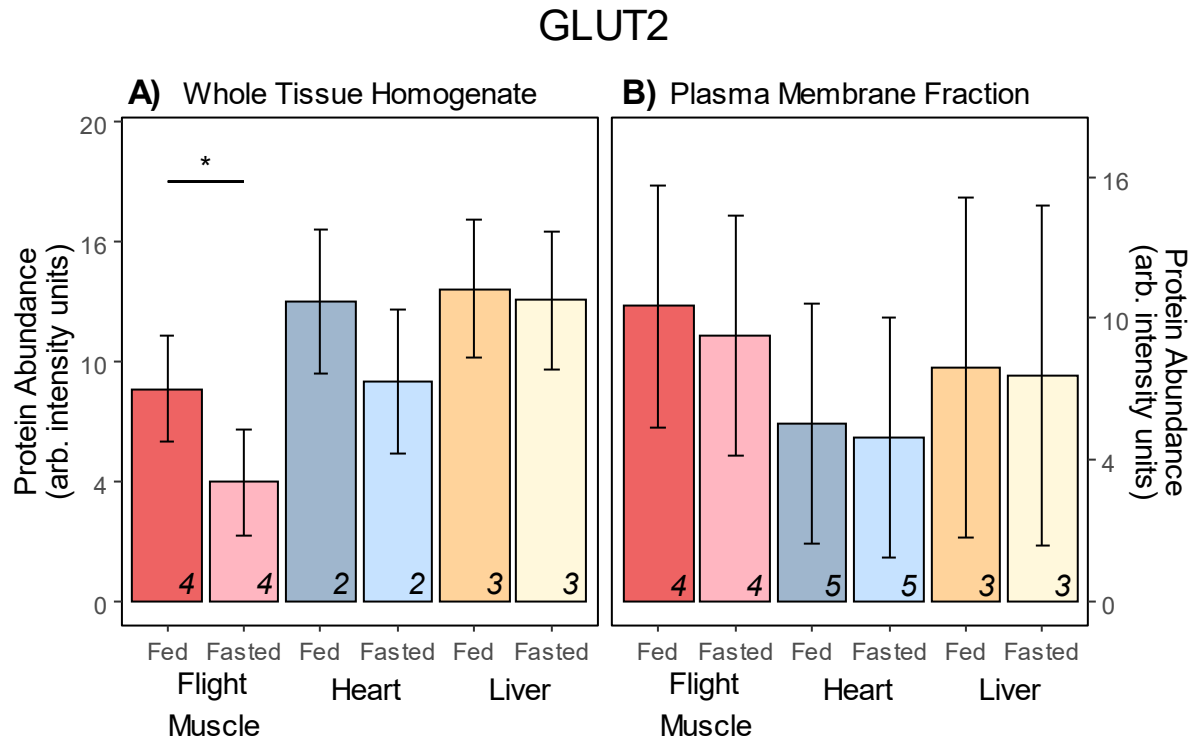
444 **Table 4: Relative abundance of GLUT1, GLUT2, GLUT3, and GLUT5 among PM**
 445 **fractions of flight muscle, heart, and liver of fed and fasted hummingbirds.** Values represent
 446 the relative abundance of GLUT proteins from isolated plasma membrane samples (fractionation
 447 efficiency approx. $92.1 \pm 0.5\%$; see Table S2). Asterisks (*) indicate $p < 0.05$.

Plasma Mem. Fraction	GLUT Isoform	Relative Fed Ratio	<i>p</i> -value	Sample Size	Relative Fasted Ratio	<i>p</i> -value	Sample Size
Flight Muscle / Heart	GLUT1	4.87 ± 1.30	0.009*	6, 4	2.48 ± 0.66	0.075	6, 5
	GLUT2	2.31 ± 2.20	0.782	4, 5	1.77 ± 1.67	0.835	4, 5
	GLUT3	1.68 ± 0.79	0.814	4, 5	1.53 ± 0.71	0.950	4, 5
	GLUT5	1.84 ± 1.18	0.451	4, 5	1.96 ± 1.24	0.318	4, 5
Flight Muscle / Liver	GLUT1	<i>Not detected in liver PM</i>			<i>Not detected in liver PM</i>		
	GLUT2	1.19 ± 1.37	0.954	4, 3	1.00 ± 1.16	0.980	4, 3
	GLUT3	0.48 ± 0.27	0.396	4, 3	0.74 ± 0.42	0.958	4, 3
	GLUT5	0.61 ± 0.47	0.976	4, 3	0.39 ± 0.30	0.747	4, 3
Heart / Liver	GLUT1	<i>Not detected in liver PM</i>			<i>Not detected in liver PM</i>		
	GLUT2	0.51 ± 0.59	0.961	5, 3	0.57 ± 0.65	0.954	5, 3
	GLUT3	0.28 ± 0.16	0.225	5, 3	0.48 ± 0.27	0.730	5, 3
	GLUT5	0.33 ± 0.25	0.643	5, 3	0.20 ± 0.15	0.747	5, 3



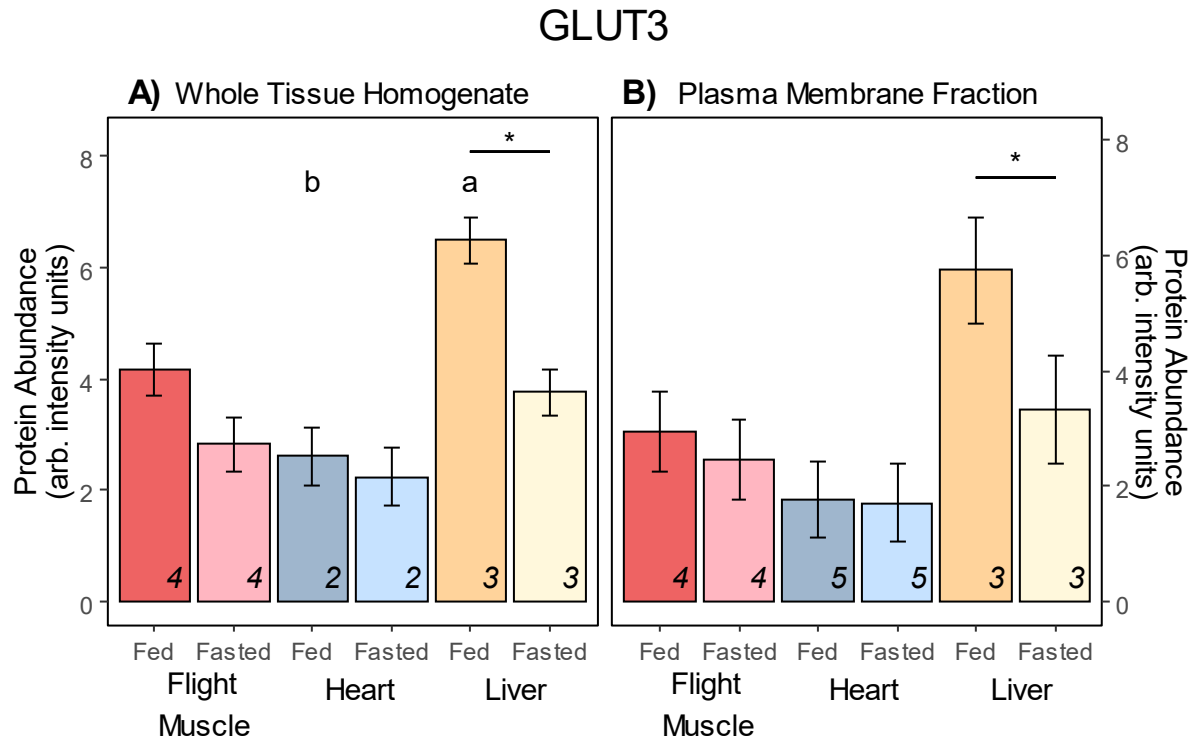
449

450 **Figure 2. Relative protein abundance of GLUT1 in hummingbird flight muscle, heart, and**
451 **liver tissue.** Data represents mean \pm standard error of arbitrary units of intensity based on
452 analyses of normalised immunoblots. *Ad-libitum* fed (“Fed”) and 1-hour fasted (“Fasted”)
453 hummingbird GLUT1 abundance was measured in A) whole tissue homogenates and B) plasma
454 membrane fraction samples. An asterisk (*) over a tissue group indicates a significant difference
455 ($p < 0.05$) of GLUT1 between fed and fasted conditions within that tissue, summarised in Table
456 1 and Table 2. Letters (a, b) over tissue groups represent a significant difference ($p < 0.05$) of
457 GLUT1 between tissue groups in fed or fasted conditions, summarised in Table 3 and Table 4.
458 Sample sizes are superimposed on the bottom-right for each tissue and treatment.



459

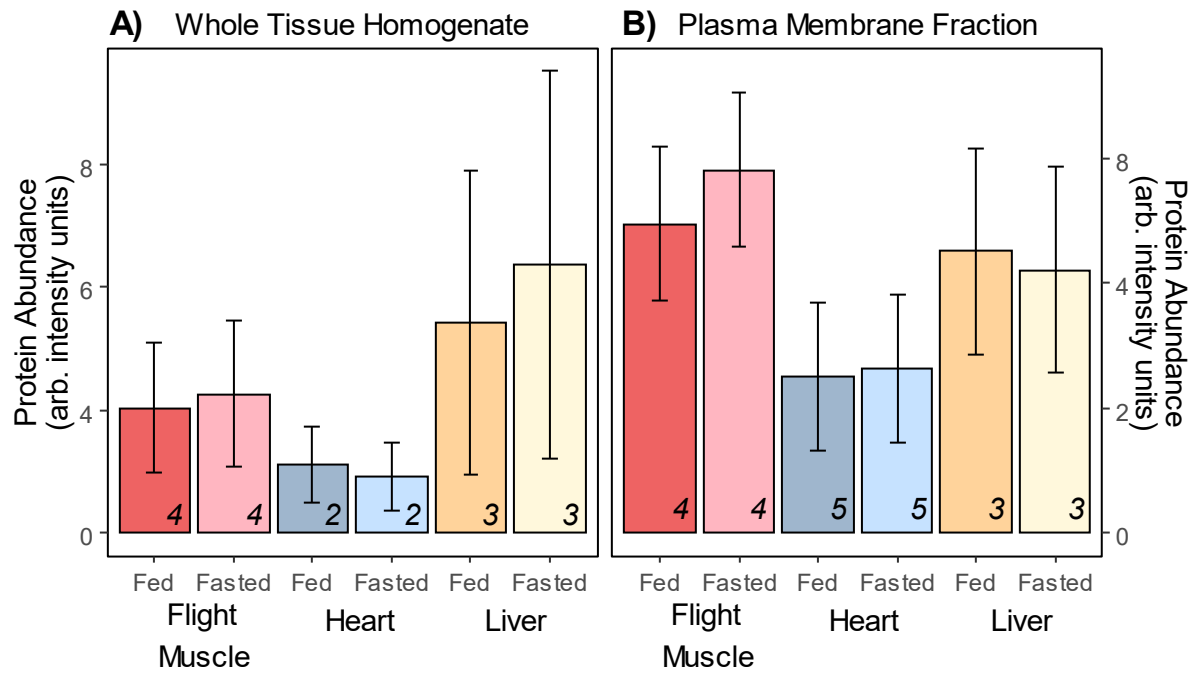
460 **Figure3. Relative protein abundance of GLUT2 in hummingbird flight muscle, heart, and**
461 **liver tissue.** Data represents mean \pm standard error of arbitrary units of intensity based on
462 analyses of normalised immunoblots. *Ad-libitum* fed (“Fed”) and 1-hour fasted (“Fasted”)
463 hummingbird GLUT2 abundance was measured in A) whole tissue homogenates and B) plasma
464 membrane fraction samples. An asterisk (*) over a tissue group indicates a significant difference
465 ($p < 0.05$) of GLUT2 between fed and fasted conditions within that tissue, summarised in Table
466 1 and Table 2. Differences in abundance of GLUT2 between tissue groups in fed or fasted
467 conditions, summarised in Table 3 and Table 4. Sample sizes are superimposed on the bottom-
468 right for each tissue and treatment.



469

470 **Figure 4. Relative protein abundance of GLUT3 in hummingbird flight muscle, heart, and**
471 **liver tissue.** Data represents mean \pm standard error of arbitrary units of intensity based on
472 analyses of normalised immunoblots. *Ad-libitum* fed (“Fed”) and 1-hour fasted (“Fasted”)
473 hummingbird GLUT3 abundance was measured in A) whole tissue homogenates and B) plasma
474 membrane fraction samples. An asterisk (*) over a tissue group indicates a significant difference
475 ($p < 0.05$) of GLUT3 between fed and fasted conditions within that tissue, summarised in Table
476 1 and Table 2. Letters (a, b) over tissue groups represent a significant difference ($p < 0.05$) of
477 GLUT3 between tissue groups in fed or fasted conditions, summarised in Table 3 and Table 4.
478 Sample sizes are superimposed on the bottom-right for each tissue and treatment.

GLUT5



479

480 **Figure 5. Relative protein abundance of GLUT5 in hummingbird flight muscle, heart, and**
481 **liver tissue.** Data represents mean \pm standard error of arbitrary units of intensity based on
482 analyses of normalised immunoblots. *Ad-libitum* fed (“Fed”) and 1-hour fasted (“Fasted”)
483 hummingbird GLUT5 abundance was measured in A) whole tissue homogenates and B) plasma
484 membrane fraction samples. Differences in GLUT5 abundance between fed and fasted
485 conditions within a given tissue are summarised in Table 1 and Table 2. Differences in overall
486 GLUT5 abundance between tissue groups in fed or fasted conditions, summarised in Table 3 and
487 Table 4. Sample sizes are superimposed on the bottom-right for each tissue and treatment.

488 Discussion

489 Following a 1-hour treatment period, hummingbirds that were fasted ($n = 5$) had significantly
490 lower blood fructose concentration compared to those that continued to feed ($n = 6$) (fed; $5.34 \pm$
491 0.24 mM, fasted; 0.21 ± 0.15 mM, $t_{9,9} = -17.2$, $p > 0.001$; Figure 1). As this is the first report of
492 blood fructose concentrations in hummingbirds, it is useful to compare our results against
493 available data from other vertebrates that specialise on sugar-rich food sources. In frugivorous
494 bats, such as the Egyptian fruit bat (*Rousettus aegyptiacus*), blood fructose concentrations are
495 known to rise to ~ 11 mM following a fructose-only meal (Keegan, 1977). Egyptian fruit bats,
496 much like hummingbirds, have been shown to rapidly incorporate fructose into their pool of
497 metabolizable substrates (Keegan, 1977). In the nectarivorous Pallas's long-tongued bat
498 (*Glossophaga soricina*), the fraction of expired CO₂ supported by labelled carbons (f_{exo}) from a
499 fructose meal takes ~ 9 minutes to reach 50% (Voigt and Speakman, 2007) while it took ruby-
500 throated hummingbirds ~ 14 minutes (Chen and Welch, 2014). In this study, we also see very low
501 blood fructose concentrations in fasted hummingbirds compared to those that were fed (Figure
502 1). We further observed a slightly higher lactate concentration in fasted hummingbirds, although
503 not significantly so (Figure 1), suggesting elevated fructolytic pathway activity (Dekker et al.,
504 2010). These results indicate a rapid depletion of circulating fructose levels and may imply the
505 rapid incorporation of exogenous blood fructose into the pool of metabolizable substrates in
506 hummingbirds entering a fast.

507 In contrast, while circulating concentrations of glucose were, as expected, high in fed
508 hummingbirds, they remained elevated in fasted hummingbirds (fed; 30.04 ± 2.03 mM, fasted;
509 29.67 ± 1.25 mM; Fig. 1). Beuchat and Chong (1998) had previously observed a similar trend in
510 hummingbirds entering a fast; blood glucose concentration remained elevated for the first hour
511 and declined only after ~ 1.5 hours of fasting. Organs such as the brain are exceptionally
512 demanding of glucose (Tokushima et al., 2005) in *gallus gallus* chicks and likely other birds as
513 well. Further, lipogenic pathways of the hummingbird liver also shows a preference for glucose
514 over fructose (Dick et al., 2019). Finally, while hummingbirds have the capacity to hover
515 oxidising either glucose-only or fructose-only meals (Chen and Welch, 2014), their flight muscle
516 cells' maximal capacity for monosaccharide phosphorylation is twice as high for glucose
517 compared to fructose in tissue homogenates *in vitro* (Myrka and Welch, 2018). As hummingbird

518 muscles lack extensive glycogen stores (Suarez et al., 1990), processes such as gluconeogenesis
519 in the liver or other tissues may underlie the maintenance of elevated blood glucose. Our
520 observations suggest that glucose uptake capacity is initially downregulated in hummingbirds
521 entering a fast while fructose uptake capacity is unchanged.

522 Control of glucose and fructose flux is well-described in avian species. Despite the absence
523 of the insulin-GLUT4 system in avian muscle cells (Dupont, 2009), chickens and English
524 sparrows (*Passer domesticus*) have demonstrated coordinated expression of GLUT isoforms to
525 control sugar transmembrane transport (Sweazea and Braun, 2006; Wagstaff and White, 1995).
526 Less is known about hummingbird GLUT expression and regulation. In this study, we detected a
527 strong immunoblot signal of the protein presence of GLUT 2, 3 and 5 in hummingbird flight
528 muscle, heart, and liver tissue in WT homogenates (Table 1). GLUT2 was observed as a doublet
529 while GLUT3 was detected at a size slightly larger than predicted, both of which may be
530 attributable to variations in glycosylation (Asano et al., 1992; Ohtsubo et al., 2013). GLUT1
531 protein was detected in hummingbird flight muscle and heart (Table S1). GLUT1 protein in WT
532 liver homogenates of ruby-throated hummingbirds was only minimally visible (Table 1) and
533 was, surprisingly, not detected in PM fractions (Table 2). This result is in contrast to previously
534 reported detection of hepatic mRNA transcript for GLUT1 in both chickens (Byers et al., 2018)
535 and hummingbirds (Welch et al., 2013). However, as GLUT1 is abundant in erythrocytes
536 (Carruthers, 2009), it is possible that the previous mRNA detection, as well as our detection of
537 some hepatic GLUT1 protein, may have resulted from red blood cell contamination. While the
538 presence of transcript does not necessarily mean that the final protein form is being fully
539 transcribed (Vogel and Marcotte, 2012), it is clear that hepatic GLUT1 is not translocated to the
540 plasma membrane. Our findings are similar to others that have failed to detect GLUT1 in the
541 avian liver (Byers et al., 2017; Carver et al., 2001), raising the possibility that the role of hepatic
542 GLUT1 protein may be much more reduced among birds than previously appreciated.

543 In chickens, GLUT protein expression appears to be dependent on synthesis or degradation
544 of protein (Yamada et al., 1983) rather than the translocation from cytosolic pools that is
545 observed in mammalian cells (Guma et al., 1995). If the same were true in hummingbirds, GLUT
546 abundance of the overall tissue should be tied to the abundance of GLUT protein in the PM. In
547 this study, we noted that flight muscle overall showed the greatest response to fasting, in terms of

548 relative WT GLUT abundance. We detected significantly lower WT GLUT1 (fasted/fed ratio:
549 0.73 ± 0.09 , $p = 0.010$, $N_{fed:fasted} = 6, 6$; Table 1 and Fig. 2A), WT GLUT2 (fasted/fed ratio:
550 0.54 ± 0.08 , $p = 0.019$, $N_{fed:fasted} = 4, 4$; Table 1 and Fig. 3A), and WT GLUT3 (fasted/fed
551 ratio: 0.68 ± 0.09 , $p = 0.015$, $N_{fed:fasted} = 4, 4$; Table 1 and Fig. 4A) in flight muscle of fasted
552 hummingbirds. While GLUTs do not contribute to transmembrane transport of sugars until they
553 are expressed in the PM, this reduction of glucose-specific WT GLUTs across the whole flight
554 muscle tissue may underlie the reduced glucose uptake capacity. This may be especially
555 important in their flight muscle as its metabolic demands overshadow that of other tissues during
556 hovering (Suarez, 1992). Heart tissue of fasted hummingbirds showed no differences in GLUT
557 abundance compared to fed hummingbirds. This muted response to fasting was expected as
558 cardiac metabolism relies predominantly on circulating triglycerides (Pascual and Coleman,
559 2016) and this may be especially true of hummingbirds as they routinely switch to fatty acid
560 metabolism during periods of fasting (Welch et al., 2018). However, it may also imply that the
561 elevated blood glucose concentration in fasted hummingbirds provides sufficient substrate for
562 cardiac metabolism, especially given hummingbirds used in this study were constrained to
563 continuously perch during the fasting period. Finally, in liver tissue, only WT GLUT3 was
564 significantly lower in fasted hummingbirds liver (fasted/fed ratio: 0.58 ± 0.09 , $p = 0.0001$, N
565 $_{fed:fasted} = 3, 3$; Table 1 and Fig. 4A). Chickens have also been shown to decrease their hepatic
566 rate of glucose metabolism when fasted (Goodridge, 1968). And considering that we did not
567 detect PM GLUT1 protein, as described previously, this reduction in GLUT3 abundance during a
568 fast in the liver might have a large effect on glucose import capacity.

569 Despite the relative abundance in WT homogenates, the functional capacity for sugar import
570 into an active cell is dependent on the density of active GLUTs expressed in the PM
571 (Wasserman, 2009). In this study, we detected significantly less PM GLUT1 protein in the flight
572 muscle (fasted/fed: 0.61 ± 0.06 , $p = 0.002$, $N_{fed:fasted} = 6, 6$; Table 2 and Fig. 2B) and PM
573 GLUT3 protein in the liver (fasted/fed ratio: 0.58 ± 0.10 , $p = 0.004$, $N_{fed:fasted} = 3, 3$; Table 2
574 and Fig 4B) of fasted hummingbirds. This study is the first to report differences in subcellular
575 abundance of GLUT protein in fed and fasted hummingbirds. Our results suggest that within the
576 first hour of a fast, hummingbirds maintain elevated blood glucose levels through the lowering of
577 glucose-specific glucose transporter abundance in the PM of these tissues. In this case, reduced

578 expression of two high-affinity glucose-specific GLUTs in the PM, GLUT1 ($K_m \approx 3\text{-}5\text{mM}$; Zhao
579 & Keating, 2007) and GLUT3 ($K_m \approx 1.5\text{mM}$; Mueckler & Thorens, 2013), may substantially
580 impact the import of glucose into flight muscle and liver tissues, respectively. As we observed
581 concordant decreases in WT GLUT1 in the flight muscle and WT GLUT3 in the liver, our data
582 suggests that hummingbirds, much like chickens, regulate PM GLUT expression via synthesis or
583 degradation of protein, rather than its translocation. Additionally, a recent study measuring levels
584 of chicken GLUT1 mRNA also noticed a decrease in transcript following fasting (Coudert et al.,
585 2018). We further observed that the fructose-transporting GLUT2 (Fig. 3B) and GLUT5 (Fig.
586 5B), did not change in PM abundance in any tissues tested following the 1-hour fast (Table 2).
587 GLUT5 abundance did not change in WT homogenates either for any tissues. This suggests that
588 PM GLUT5 and PM GLUT2 remain constitutively expressed in the PM of hummingbirds
589 entering a fast. As expression of PM GLUTs allows for rapid sugar import (Wasserman, 2009),
590 and as the highest affinity for fructose that is exhibited by GLUT5 ($K_m \approx 11\text{-}12\text{mM}$; Douard &
591 Ferraris, 2008), this constitutive expression may underlie the observed reduced blood fructose
592 concentration in fasted hummingbirds.

593 In conclusion, we detected GLUTs 1, 2, 3, and 5 in all tissues, with the exception of GLUT1
594 in the liver PM. Flight muscle was observed to respond most dynamically to a 1-hour fast,
595 followed by the liver, and finally the heart. We observed a decrease in the PM and WT
596 abundance of glucose-specific GLUT1 in flight muscle and GLUT3 in the liver, which may lead
597 to reduced glucose import capacity and thus maintenance of elevated blood glucose
598 concentrations in fasted hummingbirds. In addition, we observed the constitutive expression of
599 fructose-transporting PM GLUT2 and PM GLUT5 in all tissues, which should permit continued
600 fructose uptake into these tissue during initial stages of fasting, leading to near-depletion of the
601 circulating pool of fructose. We further observed that the changes in GLUT protein expression
602 occur both intracellularly and in the PM – no decrease of GLUT protein in the PM occurred
603 without a concordant decrease in WT homogenates. These results suggest that hummingbirds,
604 similar to other birds, may rely on mechanisms of GLUT synthesis and degradation, rather than
605 translocation, to regulate extreme fluxes in circulating glucose and fructose concentrations.

606 **Acknowledgements**

607 We would like to thank Alex Myrka for his lessons on Western blotting and Lily Hou for her
608 expertise in the development of the mixed-effects model employed in this study. We are also
609 grateful to the Welch Lab volunteers for their assistance with hummingbird capture. We extend a
610 special thanks to Rachael Sparklin and Dr. Winston Timp for assembling the hummingbird
611 transcriptome. Finally, we would like to thank Dr. Aarthi Ashok, Dr. Mauricio Terebiznik, and
612 the Welch Lab team for their insights, critiques, and support.

613 **Conflicting Interests**

614 None to declare.

615 **Funding**

616 This research was supported by grants from the Natural Sciences and Engineering Research
617 Council of Canada Discovery Grant (number 386466) to KCW and the Human Frontier Science
618 Program (number RGP0062/2016) to KCW and GWW.

619 **References**

- 620 Asano, T., Katagiri, H., Takata, K., Tsukuda, K., Lin, J.L., Ishihara, H., Inukai, K., Hirano, H.,
621 Yazaki, Y., Oka, Y., 1992. Characterization of GLUT3 protein expressed in Chinese
622 hamster ovary cells. *Biochemical Journal* 288, 189–193.
623 <https://doi.org/10.1042/bj2880189>
- 624 Bates, D., Mächler, M., Bolker, B., Walker, S., 2015. Fitting Linear Mixed-Effects Models Using
625 **lme4**. *Journal of Statistical Software* 67. <https://doi.org/10.18637/jss.v067.i01>
- 626 Beuchat, C.A., Chong, C.R., 1998. Hyperglycemia in hummingbirds and its consequences for
627 hemoglobin glycation. *Comparative Biochemistry and Physiology Part A: Molecular &*
628 *Integrative Physiology* 120, 409–416.
- 629 Boratyn, G.M., Schäffer, A.A., Agarwala, R., Altschul, S.F., Lipman, D.J., Madden, T.L., 2012.
630 Domain enhanced lookup time accelerated BLAST. *Biology Direct* 7, 12.
631 <https://doi.org/10.1186/1745-6150-7-12>
- 632 Byers, M.S., Bohannon-Stewart, A., Khwatenge, C., Alqureish, E., Alhathlol, A., Nahashon, S.,
633 Wang, X., 2018. Absolute Quantification of Tissue Specific Expression of Glucose
634 Transporters in Chickens 1, 8.
- 635 Byers, M.S., Howard, C., Wang, X., 2017. Avian and Mammalian Facilitative Glucose
636 Transporters. *Microarrays* 6, 7. <https://doi.org/10.3390/microarrays6020007>
- 637 Carruthers, A., 2009. Will the original glucose transporter isoform please stand up! *American*
638 *Journal of Physiology-Endocrinology and Metabolism* 297, E836–E848.
639 <https://doi.org/10.1152/ajpendo.00496.2009>
- 640 Carver, F.M., Shibley, Jr, I.A., Pennington, J.S., Pennington, S.N., 2001. Differential expression
641 of glucose transporters during chick embryogenesis: *Cellular and Molecular Life*
642 *Sciences* 58, 645–652. <https://doi.org/10.1007/PL00000887>
- 643 Chen, C.C.W., Welch, K.C., 2014. Hummingbirds can fuel expensive hovering flight completely
644 with either exogenous glucose or fructose. *Functional Ecology* 28, 589–600.
645 <https://doi.org/10.1111/1365-2435.12202>
- 646 Chen, K.K., 1945. Susceptibility of birds to insulin as compared with mammals. *Journal of*
647 *Pharmacology and Experimental Therapeutics* 84, 74–77.

- 648 Coudert, E., Praud, C., Dupont, J., Crochet, S., Cailleau-Audouin, E., Bordeau, T., Godet, E.,
649 Collin, A., Berri, C., Tesseraud, S., Métayer-Coustard, S., 2018. Expression of glucose
650 transporters SLC2A1, SLC2A8, and SLC2A12 in different chicken muscles during
651 ontogenesis. *Journal of Animal Science* 96, 498–509. <https://doi.org/10.1093/jas/skx084>
- 652 Dekker, M.J., Su, Q., Baker, C., Rutledge, A.C., Adeli, K., 2010. Fructose: a highly lipogenic
653 nutrient implicated in insulin resistance, hepatic steatosis, and the metabolic syndrome.
654 *American Journal of Physiology-Endocrinology and Metabolism* 299, E685–E694.
655 <https://doi.org/10.1152/ajpendo.00283.2010>
- 656 del Rio, M., Baker, H.G., Baker, I., 1992. Ecological and evolutionary implications of digestive
657 processes: Bird preferences and the sugar constituents of floral nectar and fruit pulp.
658 *Experientia* 48, 544–551. <https://doi.org/10.1007/BF01920237>
- 659 Dick, M.F., Alcantara-Tangonan, A., Shamli Oghli, Y., Welch, K.C., 2019. Metabolic
660 partitioning of sucrose and seasonal changes in fat turnover rate in ruby-throated
661 hummingbirds (*Archilochus colubris*). *J Exp Biol* jeb.212696.
662 <https://doi.org/10.1242/jeb.212696>
- 663 Douard, V., Ferraris, R.P., 2008. Regulation of the fructose transporter GLUT5 in health and
664 disease. *American Journal of Physiology-Endocrinology and Metabolism* 295, E227–
665 E237. <https://doi.org/10.1152/ajpendo.90245.2008>
- 666 Dupont, J., 2009. Insulin signaling in chicken liver and muscle. *General and Comparative*
667 *Endocrinology* 163, 52–57. <https://doi.org/10.1016/j.ygcen.2008.10.016>
- 668 Eberts, E., Dick, M., Welch, K., 2019. Metabolic Fates of Evening Crop-Stored Sugar in Ruby-
669 Throated Hummingbirds (*Archilochus colubris*). *Diversity* 11, 9.
670 <https://doi.org/10.3390/d11010009>
- 671 Egert, S., Nguyen, N., Schwaiger, M., 1999. Myocardial Glucose Transporter GLUT1:
672 Translocation Induced by Insulin and Ischemia. *Journal of Molecular and Cellular*
673 *Cardiology* 31, 1337–1344. <https://doi.org/10.1006/jmcc.1999.0965>
- 674 Gassmann, M., Grenacher, B., Rohde, B., Vogel, J., 2009. Quantifying Western blots: Pitfalls of
675 densitometry. *ELECTROPHORESIS* 30, 1845–1855.
676 <https://doi.org/10.1002/elps.200800720>
- 677 Gasteiger, E., Hoogland, C., Gattiker, A., Duvaud, S., Wilkins, M.R., Appel, R.D., Bairoch, A.,
678 2005. Protein Identification and Analysis Tools on the ExPASy Server, in: Walker, J.M.

- 679 (Ed.), *The Proteomics Protocols Handbook*. Humana Press, Totowa, NJ, pp. 571–607.
680 <https://doi.org/10.1385/1-59259-890-0:571>
- 681 Godoy, A., Ulloa, V., Rodríguez, F., Reinicke, K., Yañez, A.J., García, M. de los A., Medina,
682 R.A., Carrasco, M., Barberis, S., Castro, T., Martínez, F., Koch, X., Vera, J.C., Poblete,
683 M.T., Figueroa, C.D., Peruzzo, B., Pérez, F., Nualart, F., 2006. Differential subcellular
684 distribution of glucose transporters GLUT1–6 and GLUT9 in human cancer:
685 Ultrastructural localization of GLUT1 and GLUT5 in breast tumor tissues. *J. Cell.*
686 *Physiol.* 207, 614–627. <https://doi.org/10.1002/jcp.20606>
- 687 Guma, A., Zierath, J.R., Wallberg-Henriksson, H., Klip, A., 1995. Insulin induces translocation
688 of GLUT-4 glucose transporters in human skeletal muscle. *American Journal of*
689 *Physiology-Endocrinology and Metabolism* 268, E613–E622.
690 <https://doi.org/10.1152/ajpendo.1995.268.4.E613>
- 691 Han, J., Gagnon, S., Eckle, T., Borchers, C.H., 2013. Metabolomic analysis of key central carbon
692 metabolism carboxylic acids as their 3-nitrophenylhydrazones by UPLC/ESI-MS:
693 General. *ELECTROPHORESIS* n/a-n/a. <https://doi.org/10.1002/elps.201200601>
- 694 Han, J., Lin, K., Sequira, C., Yang, J., Borchers, C.H., 2016. Quantitation of low molecular
695 weight sugars by chemical derivatization-liquid chromatography/multiple reaction
696 monitoring/mass spectrometry: Liquid Phase Separations. *ELECTROPHORESIS* 37,
697 1851–1860. <https://doi.org/10.1002/elps.201600150>
- 698 Karasov, W.H., 2017. Integrative physiology of transcellular and paracellular intestinal
699 absorption. *The Journal of Experimental Biology* 220, 2495–2501.
700 <https://doi.org/10.1242/jeb.144048>
- 701 Keegan, D.J., 1977. Aspects of the assimilation of sugars by *Rousettus aegyptiacus*. *Comparative*
702 *Biochemistry and Physiology Part A: Physiology* 58, 349–352.
703 [https://doi.org/10.1016/0300-9629\(77\)90153-0](https://doi.org/10.1016/0300-9629(77)90153-0)
- 704 Klip, A., Volchuk, A., He, L., Tsakiridis, T., 1996. The glucose transporters of skeletal muscle.
705 *Seminars in Cell & Developmental Biology* 7, 229–237.
706 <https://doi.org/10.1006/scdb.1996.0031>
- 707 Lenth, R., 2019. emmeans: Estimated Marginal Means, aka Least-Squares Means. R package
708 version 1.4.

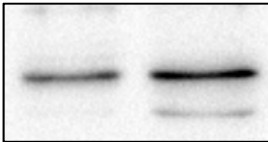
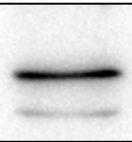
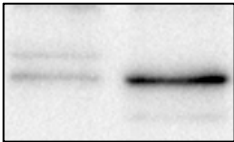
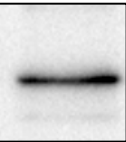
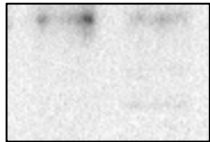
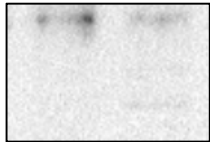
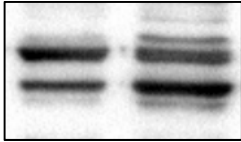
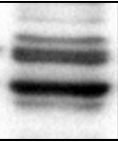
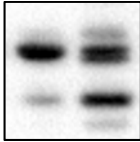

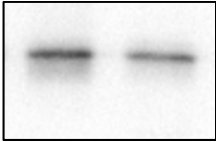
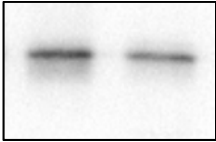
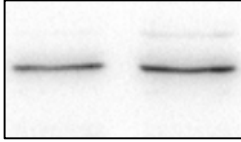
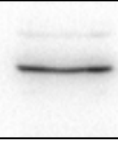
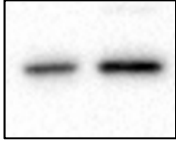

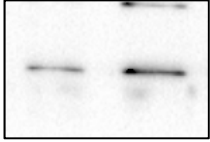
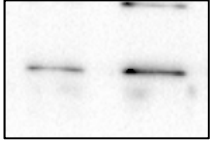
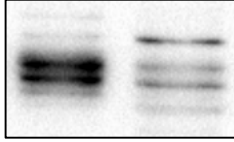
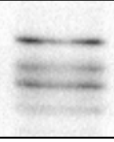
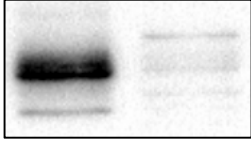
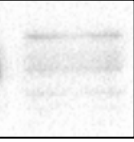
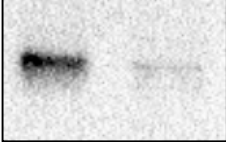
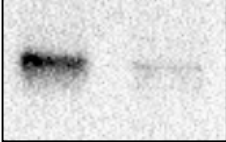
- 709 Mathieu-Costello, O., Suarez, R., Hochachka, P.W., 1992. Capillary-to-fiber geometry and
710 mitochondrial density in hummingbird flight muscle. *Respiration physiology* 89, 113–
711 132.
- 712 Mueckler, M., Thorens, B., 2013. The SLC2 (GLUT) family of membrane transporters.
713 *Molecular Aspects of Medicine* 34, 121–138. <https://doi.org/10.1016/j.mam.2012.07.001>
- 714 Myrka, A.M., Welch, K.C., 2018. Evidence of high transport and phosphorylation capacity for
715 both glucose and fructose in the ruby-throated hummingbird (*Archilochus colubris*).
716 *Comparative Biochemistry and Physiology Part B: Biochemistry and Molecular Biology*
717 224, 253–261. <https://doi.org/10.1016/j.cbpb.2017.10.003>
- 718 Ohtsubo, K., Takamatsu, S., Gao, C., Korekane, H., Kurosawa, T.M., Taniguchi, N., 2013. N-
719 glycosylation modulates the membrane sub-domain distribution and activity of glucose
720 transporter 2 in pancreatic beta cells. *Biochemical and Biophysical Research*
721 *Communications* 434, 346–351. <https://doi.org/10.1016/j.bbrc.2013.03.076>
- 722 Pascual, F., Coleman, R.A., 2016. Fuel availability and fate in cardiac metabolism: A tale of two
723 substrates. *Biochimica et Biophysica Acta (BBA) - Molecular and Cell Biology of Lipids*
724 1861, 1425–1433. <https://doi.org/10.1016/j.bbalip.2016.03.014>
- 725 Price, E.R., Brun, A., Caviedes-Vidal, E., Karasov, W.H., 2015. Digestive Adaptations of Aerial
726 Lifestyles. *Physiology* 30, 69–78. <https://doi.org/10.1152/physiol.00020.2014>
- 727 Simon, J., Rideau, N., Taouis, M., Dupont, J., 2011. Plasma insulin levels are rather similar in
728 chicken and rat. *General and Comparative Endocrinology* 171, 267–268.
729 <https://doi.org/10.1016/j.ygcen.2011.02.025>
- 730 Simpson, I.A., Dwyer, D., Malide, D., Moley, K.H., Travis, A., Vannucci, S.J., 2008. The
731 facilitative glucose transporter GLUT3: 20 years of distinction. *American Journal of*
732 *Physiology-Endocrinology and Metabolism* 295, E242–E253.
733 <https://doi.org/10.1152/ajpendo.90388.2008>
- 734 Suarez, R., 1992. Hummingbird flight: Sustaining the highest mass-specific metabolic rates
735 among vertebrates. *Experientia* 48, 565–570. <https://doi.org/10.1007/BF01920240>
- 736 Suarez, R., Brownsey, R.W., Vogl, W., Brown, G.S., Hochachka, P.W., 1988. Biosynthetic
737 capacity of hummingbird liver. *American Journal of Physiology-Regulatory, Integrative*
738 *and Comparative Physiology* 255, R699–R702.
739 <https://doi.org/10.1152/ajpregu.1988.255.5.R699>

- 740 Suarez, R., Lighton, J.R., Moyes, C.D., Brown, G.S., Gass, C.L., Hochachka, P.W., 1990. Fuel
741 selection in rufous hummingbirds: ecological implications of metabolic biochemistry.
742 *Proceedings of the National Academy of Sciences* 87, 9207–9210.
743 <https://doi.org/10.1073/pnas.87.23.9207>
- 744 Suarez, R., Welch, K., 2017. Sugar Metabolism in Hummingbirds and Nectar Bats. *Nutrients* 9,
745 743. <https://doi.org/10.3390/nu9070743>
- 746 Suarez, R., Welch, K.C., 2011. The sugar oxidation cascade: aerial refueling in hummingbirds
747 and nectar bats. *Journal of Experimental Biology* 214, 172–178.
748 <https://doi.org/10.1242/jeb.047936>
- 749 Sweazea, K.L., Braun, E.J., 2006. Glucose transporter expression in English sparrows (*Passer*
750 *domesticus*). *Comparative Biochemistry and Physiology Part B: Biochemistry and*
751 *Molecular Biology* 144, 263–270. <https://doi.org/10.1016/j.cbpb.2005.12.027>
- 752 Thorens, Mueckler, M., 2010. Glucose transporters in the 21st Century. *American Journal of*
753 *Physiology-Endocrinology and Metabolism* 298, E141–E145.
754 <https://doi.org/10.1152/ajpendo.00712.2009>
- 755 Tokushima, Y., Takahashi, K., Sato, K., Akiba, Y., 2005. Glucose uptake in vivo in skeletal
756 muscles of insulin-injected chicks. *Comparative Biochemistry and Physiology Part B:*
757 *Biochemistry and Molecular Biology* 141, 43–48.
758 <https://doi.org/10.1016/j.cbpc.2005.01.008>
- 759 Vogel, C., Marcotte, E.M., 2012. Insights into the regulation of protein abundance from
760 proteomic and transcriptomic analyses. *Nature Reviews Genetics* 13, 227–232.
761 <https://doi.org/10.1038/nrg3185>
- 762 Voigt, C.C., Speakman, J.R., 2007. Nectar-feeding bats fuel their high metabolism directly with
763 exogenous carbohydrates. *Funct Ecology* 21, 913–921. <https://doi.org/10.1111/j.1365-2435.2007.01321.x>
- 764
- 765 Wagstaff, P., White, M.K., 1995. Characterization of the Avian GLUT1 Glucose Transporter:
766 Differential Regulation of GLUT1 and GLUT3 in Chicken Embryo Fibroblasts.
767 *Molecular Biology of the Cell* 6, 15.
- 768 Wasserman, D.H., 2009. Four grams of glucose. *American Journal of Physiology-Endocrinology*
769 *and Metabolism* 296, E11–E21. <https://doi.org/10.1152/ajpendo.90563.2008>

- 770 Wasserman, D.H., Kang, L., Ayala, J.E., Fueger, P.T., Lee-Young, R.S., 2011. The physiological
771 regulation of glucose flux into muscle in vivo. *Journal of Experimental Biology* 214,
772 254–262. <https://doi.org/10.1242/jeb.048041>
- 773 Welch, K.C., Allalou, A., Sehgal, P., Cheng, J., Ashok, A., 2013. Glucose Transporter
774 Expression in an Avian Nectarivore: The Ruby-Throated Hummingbird (*Archilochus*
775 *colubris*). *PLoS ONE* 8, e77003. <https://doi.org/10.1371/journal.pone.0077003>
- 776 Welch, K.C., Myrka, A.M., Ali, R.S., Dick, M.F., 2018. The Metabolic Flexibility of Hovering
777 Vertebrate Nectarivores. *Physiology* 33, 127–137.
778 <https://doi.org/10.1152/physiol.00001.2018>
- 779 Wood, I.S., Trayhurn, P., 2003. Glucose transporters (GLUT and SGLT): expanded families of
780 sugar transport proteins. *British Journal of Nutrition* 89, 3.
781 <https://doi.org/10.1079/BJN2002763>
- 782 Workman, R.E., Myrka, A.M., Wong, G.W., Tseng, E., Welch, K.C., Timp, W., 2018. Single-
783 molecule, full-length transcript sequencing provides insight into the extreme metabolism
784 of the ruby-throated hummingbird *Archilochus colubris*. *GigaScience* 7.
785 <https://doi.org/10.1093/gigascience/giy009>
- 786 Yamada, K., Tillotson, L.G., Isselbacher, K.J., 1983. Regulation of Hexose Carriers in Chicken
787 Embryo Fibroblasts. *The Journal of Biological Chemistry* 258, 9786–9792.
- 788 Yamamoto, N., Yamashita, Y., Yoshioka, Y., Nishiumi, S., Ashida, H., 2016. Rapid Preparation
789 of a Plasma Membrane Fraction: Western Blot Detection of Translocated Glucose
790 Transporter 4 from Plasma Membrane of Muscle and Adipose Cells and Tissues. *Curr*
791 *Protoc Protein Sci.* 85:29, 1–29.
- 792 Yang, J., Holman, G., D., 1993. Comparison of GLUT4 and GLUT 1 Subcellular Trafficking in
793 Basal and Insulin-stimulated 3T3-L1 Cells. *The Journal of Biological Chemistry* 268,
794 4600–4603.
- 795 Zhang, W., Sumners, L.H., Siegel, P.B., Cline, M.A., Gilbert, E.R., 2013. Quantity of glucose
796 transporter and appetite-associated factor mRNA in various tissues after insulin injection
797 in chickens selected for low or high body weight. *Physiological Genomics* 45, 1084–
798 1094. <https://doi.org/10.1152/physiolgenomics.00102.2013>

- 799 Zhao, F.Q., Glimm, D.R., Kennelly, J.J., 1993. Distribution of mammalian facilitative glucose
800 transporter messenger rna in bovine tissues. *International Journal of Biochemistry* 25,
801 1897–1903. [https://doi.org/10.1016/0020-711X\(88\)90322-9](https://doi.org/10.1016/0020-711X(88)90322-9)
- 802 Zhao, F.Q., Keating, A.F., 2007. Functional Properties and Genomics of Glucose Transporters.
803 *Current Genomics* 8, 113–128.
- 804

805 **Supplementary Materials**
806 3.1 Custom antibodies: GLUT1, 2, 3, and 5 detection in PM and WT homogenates
807 **Table S1: GLUTs 1, 2, 3, and 5 observed molecular weights in plasma membrane (PM)**
808 **fractions and whole-tissue (WT) homogenates of flight muscle, heart, and liver.**
809 Representative immunoblots are shown for each tissue and fraction.

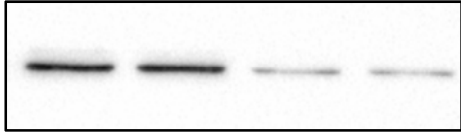
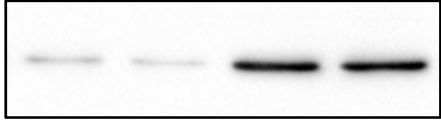
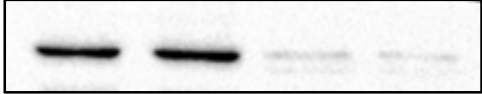
Observed Molecular Weight	Flight Muscle		Heart		Liver	
	PM	WT	PM	WT	PM	WT
GLUT1 Predicted mW = 53.8 kDa	47.0 kDa →					
						
GLUT2 Predicted mW = 57.9 kDa	43.5 kDa →					
						
GLUT3 Predicted mW = 53.3 kDa	72.4 kDa →					
						
GLUT5 Predicted mW = 56.9 kDa	55.3 kDa →					
						

811 3.2 Plasma Membrane Fractionation Purity

812 **Table S2: Relative distribution of known cytosolic or PM-residing proteins following PM**

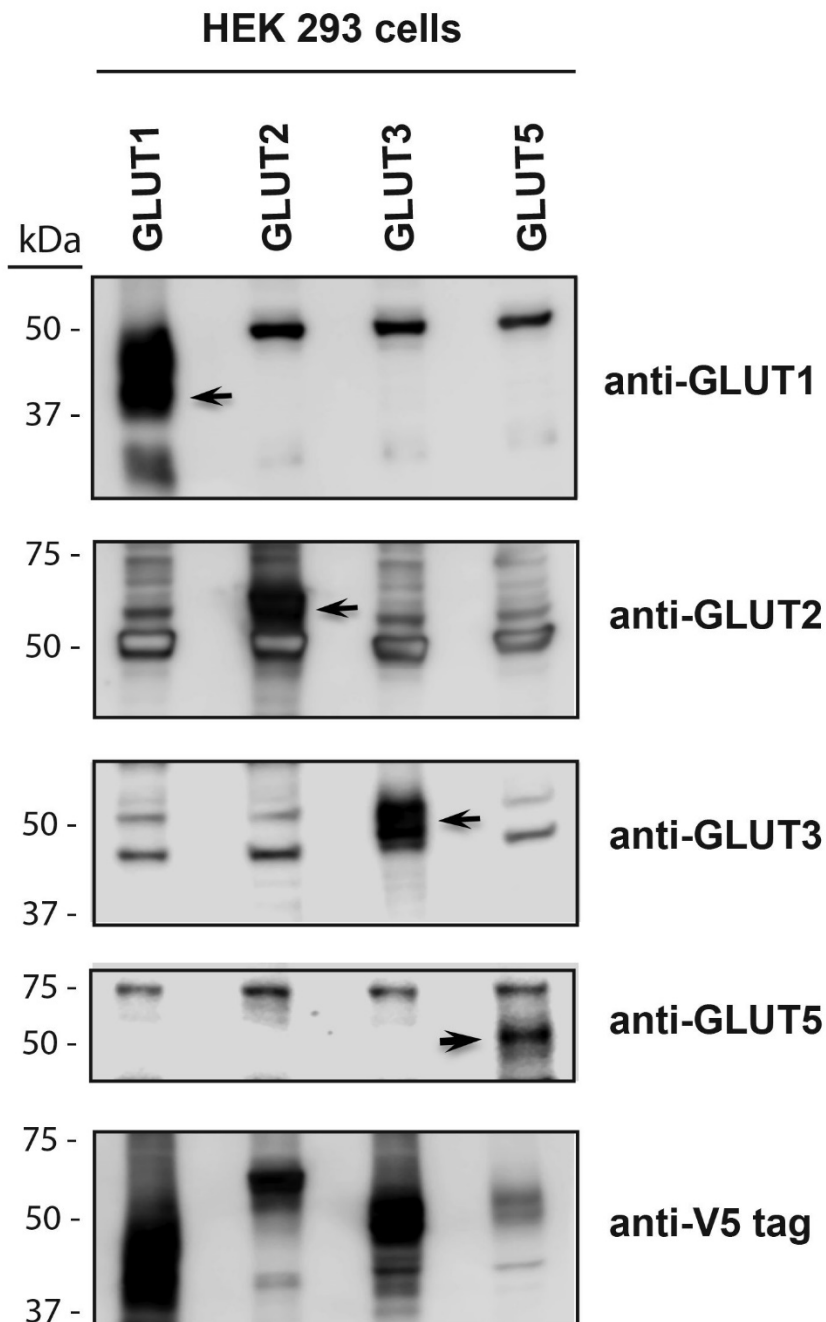
813 **fractionation.** Fraction purity indicates the relative abundance of protein in either the PM-only

814 fraction compared to the without-PM-fraction (i.e. cytosolic proteins only).

	Observed Molecular Weight	Plasma Membrane Fraction	Cytosolic Fraction (PM proteins removed)
E-Cadherin (PM-residing protein)	74.3kDa →		
Fraction staining intensity:		92.1 ± 1.8 %	7.9 ± 1.8 %
GAPDH (cytosolic protein)	34.9 kDa →		
Fraction staining intensity:		5.9 ± 0.5 %	94.1 ± 0.5 %
Na⁺/K⁺ ATPase (PM-residing protein)	103.1 kDa →		
Fraction staining intensity:		92.1 ± 0.5 %	7.8 ± 0.5 %

816 3.3 GLUT Amino Acid Sequence and Antibody Epitope

817 **Table S3: Immunoblots on lysates of overexpressed GLUT1, GLUT2, GLUT3, GLUT5**
818 **protein.** Each immunoblot lane represents a cell lysate produced from an entire well of a 6-well
819 cell-culture dish. Isoform specificity was tested via immunoblotting all cell lysates (empty vector
820 control, acGLUT1, 2, 3, and 5) with each novel GLUT antibody and observing GLUT protein
821 signal overlap.



823 **Table S4: Ruby-throated hummingbird specific GLUT1, GLUT2, GLUT3 and GLUT5**
824 **protein sequences.** Highlighted regions indicated epitope targeted during antibody development
825 to ensure greatest dissimilarity between targeted isoforms

Protein/Gene	Amino Acid Sequence
GLUT1/SLC2A1	METGSKMTARLMLAVGGAVLGSQFGYNTGVINAPQKVIEDFYNRTWLRYEETPITSATLTT LWLSVAIFSVGGMVGSFSVGLFVNRFRNSMLMSNILAFLAAVLMGFSKMALSFEMLL GRFIIGLYSGLTTGFVPMYVGEVSPTALRGALGTFHQGLGIVLGILVAQVFLDLIMGNDLWLP LLLGFIIVPALLQCIILPFAPESPRFLLINRNEENKAKSVLKKLRGTTDVSDDLQEMKEESRQMM REKKVTIMELFRSPMYRQPILIAIVLQLSQQLSGINAVFYSTIFEFKSGVEQPYYATIGSGVNT AFTVVSLFVVERAGRRTLHLIGLAGMAGCAVLMTIALTLDDQMPWMSYLSIVAIFGFVAFPEI GPGPIWPFIVAELFSQGPRAAFVAVAGLSNWTSNFIVGMGFQYIAQLCGSYVFIIFTVLLILFFI FTYFKVPETKGRTFDEIA SGFRQGGAGQSDKTPDEFHS LGADSQV <i>NCBI Accession Number: MT472837</i>
GLUT2/SLC2A2	MDKKNKMQAQEKHLTGLVLSVFAAVLGGFQYGYSLGVINAPQKVEAHYGRVLGIAPPDRFP TSASEEDGTVPVTEPWVSTEARLAPEDDPGEDLGTSSHILTMYSLSVSMFAVGGMVSSFT VGWIGDRLGRVKAMLVNVNLSIIGNLLMGLAKFGPSHMLIAGRAVTGLYCGLSGLVPMYVS EVSPTALRGALGTLHQLAIVTGILISQVLGLDFLLGNDEMWPPLLGLSGVAALLQFFLLLLCPES PRYLYIKLGKVEEAKKSLKRLRGNCNCPMKEIAEMEKEKQEAASEKKVSIRQLFTSSKYQAVIVA LMVQISQQFSGINAIFYSTNIFERAGVDQPVYATIGVGVVNTVFTVISVFLVEKAGRRSLFLA GLMGMLISAVAMTVGLALLSKFAWMSYVSMIAIFLVIFFEVGGPIWPFIVAELFSQGPRA AIATAGFCNWACNFIVGMCFQYIADLCGPYVVFIFAALLLIFFLFAYFKVPETKKGKSFEEIAAVF RRRKLPTKAMTELEDLRGEEA <i>NCBI Accession Number: MT472838</i>
GLUT3/SLC2A3	FLQKITPLVYAVSIAAIGSLQFGYNTGVINAPEKIIQAFFNRTLSESRGSEVVSSELLTSLWLSVA IFSVGGMIGSFSVSLFVNRFRNSMMLLVNLAFAAGVLMALSKLVKAVEMLIVGRFIIGIFCG LSTGFVPMYISEVSPTSLRGAFGLNQLGIVVGLVAQIFGLEAIMGTETLWPLLGFVLPVAVL QCVGLLFCPESPRFLLINKVEEKAQAVLQKLRGTEDVSQDIQEMKEESAKMSQEKKVTPEL FRSPSYRQAIIIAIMLQLSQQLSGINAVFYSTGIFERAGITKPVYATIGAGVVNTVFTVVSLFLV ERAGRRTLHLVGLGGMALCTVLMTIALALRDSVEWIKYISIIATFGFVALFEIGPGPIWPFIVA LFSQGPRAAMAVAGCSNWTSNFLVGLLFPYAEKLLGSYVFLVFLVFLVIFVFTFFKVPETKG RTFEDI SRGFEGRGDASSPSPVEKVE LSNIEAEKVA <i>NCBI Accession Number: MT472839</i>
GLUT5/SLC2A5	M KLKGGKHESDNDGSK GMTLTALVALISAFGASFQYGYNVSVINSPAPFMQEFYNQTY YRNGEYMSSEFQTLWLSLTVSMFPLGGLFGSLMVWPLVNNCGRKGTLINNIFSIVAAVLM GTSEIAKTFEVIILSRVIMGIYAGLASNVVPMFLGELSPKNLRGAIGVVPQLFITVGLSAQILGL NSILGNAAGWPILLGLTGIPSLQIQLLPLFPESPRYLLIQKGNEEQARQALQRLRGCDVYDEI EEMRREDESEKKEGQFSVLSLFTFRGLRWQLISIIVMMMGQQLSGINAVFYADRFQSGAV DTNSVQYVTVSIGAINVWMTLLAVFIIESLGRRIILLAGFGLCCLSCAVLTALNLQNTVTWMS YISIVCVIYIIGHAIGASPIPSVLITEMFLQSSRPAAFMVGGSVHWLSNFTVGLLFLYMEAGLG PYSFLIFCAICLATIYIFIVVPETKNTKTFMEINRIMAKRNKVEIQEDKDELKDFHTAPGGQAGKT VSSSEL <i>NCBI Accession Number: MT472840</i>

827 3.4 AIC Scores

828 **Table S5: Akaike information criterion (AIC) and AIC with corrections for small sample**
 829 **size (AICc) scores presented for each GLUT isoform model.** Due to a relatively small sample
 830 size, AICc was preferred over AIC. Models with the lowest AICc score were selected for post
 831 hoc analysis and are indicated with an asterisk (*). The models tested are as follows:

832 1: *Fluorescence Intensity* ~ *Treatment* + *Blot*

833 2: *Fluorescence Intensity* ~ *Tissue* + *Blot*

834 3: *Fluorescence Intensity* ~ *Treatment* + *Tissue* + *Blot*

835 4: *Fluorescence Intensity* ~ *Treatment* × *Tissue* + *Blot*

GLUT	Model	AIC Score	AICc Score	AIC Score	AICc Score
		WT	WT	PM	PM
GLUT1	1	515	519	31.9	34.4
	2	516	519	23.9	26.4
	3	479	485	25.2	29.2
	4	446	455*	17.4	23.4*
GLUT2	1	604	607	812	814
	2	570	575	773	776
	3	532	540	740	745
	4	462	478*	675	685*
GLUT3	1	270	273	373	375
	2	262	267	356	360
	3	238	246	341	346
	4	208	224*	308	318*
GLUT5	1	297	300	809	811
	2	278	283	770	773
	3	264	272	739	744
	4	234	250*	673	682*

837 3.5 Mammalian and Avian GLUT Homology

838 **Table S6: Comparison of known avian GLUT isoforms and their homology to humans.**

839 Data was aggregated from (M. S. Byers et al., 2017; Myrka & Welch, 2018; Sweazea & Braun,
840 2006; Kenneth C. Welch et al., 2013) and homology to humans was calculated using NCBI
841 BLAST (Boratyn et al., 2012).

GLUT	Localisation	Feature	Chicken to hummingbird sequence homology	Chicken to human sequence homology	Hummingbird to human sequence homology	Substrates (mammals)
GLUT1	Ubiquitous	Basal glucose transport	98%	80%	88%	Galactose, mannose, glucosamine
GLUT2	Liver, Pancreas, Intestine, Kidney	Insulin dependent	89%	65%	64%	Fructose, Glucose, Galactose
GLUT3	Neurons, Liver, skeletal muscle	Insulin dependent	87%	70%	73%	Glucose
GLUT4	Not found	Absence	N/A	N/A	N/A	Glucose
GLUT5	Intestine, brain, adipocytes, testes, skeletal muscle	Fructose transport	81%	64%	66%	Fructose

843	Figure Legends	
844	Figure 1: Mean concentrations (mM) ± standard error of circulating sugars A) Glucose, B)	
845	Fructose from plasma samples and metabolites C) Lactate, D) Pyruvate from whole-tissue	
846	homogenates of fed (n = 6) and fasted (n = 5). Data is presented as mean concentration in	
847	millimolar ± standard error. Asterisk (*) indicates $p < 0.05$	18
848	Figure 2. Relative protein abundance of GLUT1 in hummingbird flight muscle, heart, and	
849	liver tissue. Data represents mean ± standard error of arbitrary units of intensity based on	
850	analyses of normalised immunoblots. <i>Ad-libitum</i> fed (“Fed”) and 1-hour fasted (“Fasted”)	
851	hummingbird GLUT1 abundance was measured in A) whole tissue homogenates and B) plasma	
852	membrane fraction samples. An asterisk (*) over a tissue group indicates a significant difference	
853	($p < 0.05$) of GLUT1 between fed and fasted conditions within that tissue, summarised in Table	
854	1 and Table 2. Letters (a, b) over tissue groups represent a significant difference ($p < 0.05$) of	
855	GLUT1 between tissue groups in fed or fasted conditions, summarised in Table 3 and Table 4.	
856	Sample sizes are superimposed on the bottom-right for each tissue and treatment.....	22
857	Figure 3. Relative protein abundance of GLUT2 in hummingbird flight muscle, heart, and	
858	liver tissue. Data represents mean ± standard error of arbitrary units of intensity based on	
859	analyses of normalised immunoblots. <i>Ad-libitum</i> fed (“Fed”) and 1-hour fasted (“Fasted”)	
860	hummingbird GLUT2 abundance was measured in A) whole tissue homogenates and B) plasma	
861	membrane fraction samples. An asterisk (*) over a tissue group indicates a significant difference	
862	($p < 0.05$) of GLUT2 between fed and fasted conditions within that tissue, summarised in Table	
863	1 and Table 2. Differences in abundance of GLUT2 between tissue groups in fed or fasted	
864	conditions, summarised in Table 3 and Table 4. Sample sizes are superimposed on the bottom-	
865	right for each tissue and treatment.	23
866	Figure 4. Relative protein abundance of GLUT3 in hummingbird flight muscle, heart, and	
867	liver tissue. Data represents mean ± standard error of arbitrary units of intensity based on	
868	analyses of normalised immunoblots. <i>Ad-libitum</i> fed (“Fed”) and 1-hour fasted (“Fasted”)	
869	hummingbird GLUT3 abundance was measured in A) whole tissue homogenates and B) plasma	
870	membrane fraction samples. An asterisk (*) over a tissue group indicates a significant difference	

871 (p < 0.05) of GLUT3 between fed and fasted conditions within that tissue, summarised in Table
872 1 and Table 2. Letters (a, b) over tissue groups represent a significant difference (p < 0.05) of
873 GLUT3 between tissue groups in fed or fasted conditions, summarised in Table 3 and Table 4.
874 Sample sizes are superimposed on the bottom-right for each tissue and treatment..... 24

875 **Figure 5. Relative protein abundance of GLUT5 in hummingbird flight muscle, heart, and**
876 **liver tissue.** Data represents mean ± standard error of arbitrary units of intensity based on
877 analyses of normalised immunoblots. *Ad-libitum* fed (“Fed”) and 1-hour fasted (“Fasted”)
878 hummingbird GLUT5 abundance was measured in A) whole tissue homogenates and B) plasma
879 membrane fraction samples. Differences in GLUT5 abundance between fed and fasted
880 conditions within a given tissue are summarised in Table 1 and Table 2. Differences in overall
881 GLUT5 abundance between tissue groups in fed or fasted conditions, summarised in Table 3 and
882 Table 4. Sample sizes are superimposed on the bottom-right for each tissue and treatment. 25

883

884 **Table 1: Relative abundance of GLUT1, GLUT2, GLUT3, and GLUT5 in flight muscle,**
885 **heart, and liver of fed and fasted hummingbirds. Data and representative immunoblots are**
886 **presented here for the whole tissue (WT) homogenates of hummingbird tissue.** Fasted/Fed
887 ratio values represent how much change in GLUT protein abundance was detected in the fasting
888 treatment. Observed molecular weights are reported (M.W.). Sample sizes are given for the
889 number of 1) fed hummingbirds, 2) fasted hummingbirds. Asterisks (*) indicate p < 0.05. 19

890 **Table 2: Relative abundance of GLUT1, GLUT2, GLUT3, and GLUT5 in flight muscle,**
891 **heart, and liver of fed and fasted hummingbirds.** Data and representative immunoblots are
892 presented here for hummingbird tissue samples that underwent plasma membrane fractionation;
893 only PM-residing GLUTs are presented. Fasted/Fed ratio values represent how much change in
894 GLUT protein abundance was detected in the fasting treatment. Observed molecular weights are
895 reported (M.W.). Sample sizes are given for the number of 1) fed hummingbirds, 2) fasted
896 hummingbirds. Asterisks (*) indicate p < 0.05..... 20

897 **Table 3: Relative abundance of GLUT1, GLUT2, GLUT3, and GLUT5 among WT**
898 **homogenates compared pair-wise between flight muscle, heart, and liver of fed and fasted**

899	hummingbirds. Data represents the relative whole-tissue GLUT abundance. Asterisks (*)	
900	indicate $p < 0.05$	21
901	Table 4: Relative abundance of GLUT1, GLUT2, GLUT3, and GLUT5 among PM	
902	fractions of flight muscle, heart, and liver of fed and fasted hummingbirds. Values represent	
903	the relative abundance of GLUT proteins from isolated plasma membrane samples (fractionation	
904	efficiency approx. $92.1 \pm 0.5\%$; see Table.S2). Asterisks (*) indicate $p < 0.05$	21
905		
906	Table S1: GLUTs 1, 2, 3, and 5 observed molecular weights in plasma membrane (PM)	
907	fractions and whole-tissue (WT) homogenates of flight muscle, heart, and liver.	
908	Representative immunoblots are shown for each tissue and fraction.	38
909		
910	Table S2: Relative distribution of known cytosolic or PM-residing proteins following PM	
911	fractionation. Fraction purity indicates the relative abundance of protein in either the PM-only	
912	fraction compared to the without-PM-fraction (i.e. cytosolic proteins only).	39
913		
914	Table S3: Immunoblots on lysates of overexpressed GLUT1, GLUT2, GLUT3, GLUT5	
915	protein. Each immunoblot lane represents a cell lysate produced from an entire well of a 6-well	
916	cell-culture dish. Isoform specificity was tested via immunoblotting all cell lysates (empty vector	
917	control, acGLUT1, 2, 3, and 5) with each novel GLUT antibody and observing GLUT protein	
918	signal overlap.	40
919		
920	Table S4: Ruby-throated hummingbird specific GLUT1, GLUT2, GLUT3 and GLUT5	
921	protein sequences. Highlighted regions indicated epitope targeted during antibody development	
922	to ensure greatest dissimilarity between targeted isoforms	41
923		
924	Table S5: Akaike information criterion (AIC) and AIC with corrections for small sample	
925	size (AICc) scores presented for each GLUT isoform model. Due to a relatively small sample	
926	size, AICc was preferred over AIC. Models with the lowest AICc score were selected for post	
927	hoc analysis and are indicated with an asterisk (*). The models tested are as follows:	42

928	Table S6: Comparison of known avian GLUT isoforms and their homology to humans.	
929	Data was aggregated from (M. S. Byers et al., 2017; Myrka & Welch, 2018; Sweazea & Braun,	
930	2006; Kenneth C. Welch et al., 2013) and homology to humans was calculated using NCBI	
931	BLAST (Boratyn et al., 2012).....	43
932		